Review

Stan Majewski*

Perspectives of brain imaging with PET systems

https://doi.org/10.1515/bams-2021-0178
Received November 15, 2021; accepted November 17, 2021;
published online December 22, 2021

Abstract: In this partial review and partial attempt at vision of what may be the future of dedicated brain PET scanners, the key implementations of the PET technique, we postulate that we are still on a development path and there is still a lot to be done in order to develop optimal brain imagers. Optimized for particular imaging tasks and protocols, and also mobile, that can be used outside the PET center, in addition to the expected improvements in sensitivity and resolution. For this multi-application concept to be more practical, flexible, adaptable designs are preferred. This task is greatly facilitated by the improved TOF performance that allows for more open, adjustable, limited angular coverage geometries without creating image artifacts. As achieving uniform very high resolution in the whole body is not practical due to technological limits and high costs, hybrid systems using a moderate-resolution total body scanner (such as J-PET) combined with a very high performing brain imager could be a very attractive approach. As well, as using magnification inserts in the total body or long-axial length imagers to visualize selected targets with higher resolution. In addition, multigamma imagers combining PET with Compton imaging should be developed to enable multi-tracer imaging.

Keywords: brain imaging; molecular imaging; PET; spatial resolution; Time of Flight.

Introduction

This article is not an attempt at another inclusive review paper on PET brain imagers. This is more like a vision and prediction on the development trajectory (or rather trajectories) of the dedicated brain imagers, based on the assessment of the current status and opinions and visions of many members of the imaging community. Unavoidably, bias is present based on the extensive yet selected knowledge and also participation of the author in development of the dedicated PET brain imagers.

While there are sometimes different interpretations of the term "Molecular Imaging", in human imaging due to basic physics rules of radiation collimation, transmission (with diffusion/scatter) and detection, only higher energies of gamma rays can be candidates for penetrating radiation used in human imaging. As collimation and therefore spatial resolution gets worse with increasing gamma ray energy, electronic collimation in the case of pairs of back-to-back annihilation 511 keV photons produced in Positron Emission Tomography (PET) is the best technique to achieve high tissue penetration, high spatial resolution, and high sensitivity [1–10]. Recently also with ever better TOF performance [11–17]. It is also expected that in the not-so-distant future the dynamic/kinetic/parametric PET imaging will become the new PET standard.

PET is an ***excellent and proven modality in imaging cancer, dementia,*** and many other brain neuro diseases [18–29]. However, this nuclear medicine modality suffers from the stigma of radiation exposure to all organs of the human body independently of the organ to be imaged as the introduction of the radioactive imaging "contrast" agent into the body is systemic and distributed through the blood stream, therefore independently of the organ of interest and the rationale for the scan, all organs are exposed, and some are more sensitive to radiation than other.

Recently, the revolutionary Total Body PET [30–46] concept was introduced and several prototypes were built. Two companies: United Imaging and Siemens are now offering devices in that category, United's uEXPLORER is about 2 m long, and Siemens' Biograph QUADRA about 1 m long. This is an inspiration to all who develop PET scanners, including the dedicated brain PET scanners.

The need to develop dedicated PET brain imagers was driven by the fact that the standard whole body PET scanners are not optimized for brain imaging (Figure 1). Indeed, both sensitivity and spatial resolution are suboptimal for many of the brain imaging tasks. Most of the emitted brain radiation from uptake of imaging agents escapes undetected in the standard multi-ring PET scanners placed far away from the patient's head (Figure 1).

***Corresponding author: Stan Majewski**, Department of Biomedical Engineering, University of California, Davis, CA, USA,
E-mail: smajewski@ucdavis.edu

In addition, many brain imaging applications could benefit from the availability of mobile, portable, and recently also wearable compact systems, as opposed to the large bulky bolted-to-the-floor conventional PET scanners with patients placed on scanning tables in horizontal (supine or prone) positions. In addition, standard PET scanners are not optimized for dynamic operation with kinetic analysis that offers new levels of diagnostic precision. This seriously limits application of this powerful molecular imaging modality for example in screening for and early detection as well as development of treatment for Alzheimer's, in stroke and TBI rehabilitation, in depression, etc. As an example, in Switzerland the yearly allowable maximum dose from nuclear medicine/CT scans in non-cancer cases (like dementia) is 5milliSieverts (mSv). This is about the dose ***delivered by a single*** PET/CT scan using conventional PET/CT scanner.

Fortunately, due to the recent technological breakthroughs in PET instrumentation using compact solid -state-based Silicon Photomultiplier (SiPM) technology, and the progress with 3D image reconstruction algorithms, as well as with dynamic/kinetic data analysis algorithms, it became possible to design MRI-compatible Time-of-Flight (TOF) capable high-resolution brain PET imagers with ***an order of magnitude higher sensitivity*** in brain imaging than the standard whole body PET scanner in the brain imaging tasks. In addition, with the excellent now achievable TOF resolutions of down to ~200 ps FWHM, an accompanying standard CT scan providing attenuation map for the PET reconstructions (that also adds to the overall radiation dose burden) may be avoided. Recently an excellent compilation of dedicated brain PET scanners was published (related to the development of the CareMiBrain commercial system) [47].

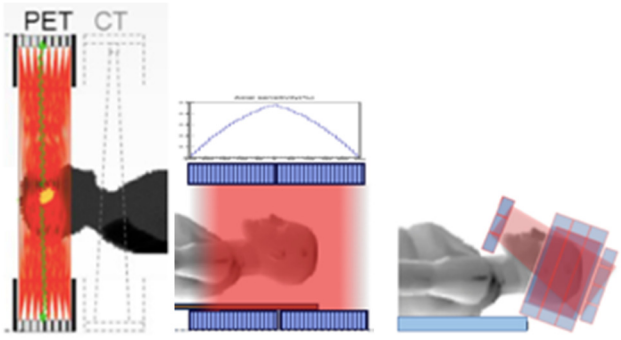

Figure 1: Two major geometries of the dedicated brain PET imagers shown in comparison with the standard brain imaging geometry (shown at left) of the clinical PET/CT scanner. At right is shown an example of a tight compact helmet design. The shown here robust TopHat compact helmet-style imager, unlike other helmet designs, avoids curved surfaces at top and bottom. Two planar detector panels, above and below the head, are added to the central multi-ring cylinder section. The mini-Explorer-type approach, used in NeuroExplorer, is shown in the center. This cylindrical design has about 50 cm axial length, and about 50 cm inner diameter.

Achieving the lowest dose operation would be only possible for tasks not requiring high spatial resolution, due to limited event statistics acquired al low injected doses. It would be rather pattern imaging than small lesion imaging to be consistent with the goal of achieving the lowest dose of about 1% of the standard dose. Also, dynamic analysis in addition to standard static imaging protocols, requires enough spatial voxel statistics and cannot operate with too small voxels. As well investigation of new analytical dynamic/kinetic algorithm approaches will be necessary. However, while the imager is primarily intended for the above listed low dose imaging tasks, it will be designed to be also able to operate at higher doses, closer to the conventional dose range.

To maximize the sensitivity, the compact tight helmet design can be used with additional top and chin region TOF PET modules to have whole brain coverage. The leading implementation design will also have option for an upright geometry to allow for long dynamic scans with high level of patient comfort and with facilitated motion correction. Different mechanical mount options are considered, some even wearable with intelligent (robotic) zero-gravity support that would automatically provide limited head motion tolerance, and some more conventional with optical monitoring system and software motion correction. Another mechanical adapter will allow the imager to be used on patients in the supine position.

Theoretically, to achieve high sensitivity in brain/head imaging, the design should: (1) provide high angular 3D coverage in the whole head; (2) implement as small as practical diameter detector structure; (3) use thick high stopping power fast scintillators to achieve high stopping power; and operate with (4) good TOF as an additional sensitivity boosting parameter. Several theoretical simulations, especially the ones performed in Refs. [48–50] and a few others have shown that **tight detector geometries following the shape of the head** with add-on top and under-the-chin or at the back-of-the-head modules are boosting significantly the detection sensitivity especially at the top and bottom regions of the brain.

However, such a design is very difficult or even impossible to fully implement using practically sized detector modules (Figure 2).

Arranging the array of such modules on a 3D spherical surface is very challenging and results necessarily in many mechanical/angular breaks that decrease the angular coverage and in addition can be the source of artifacts in

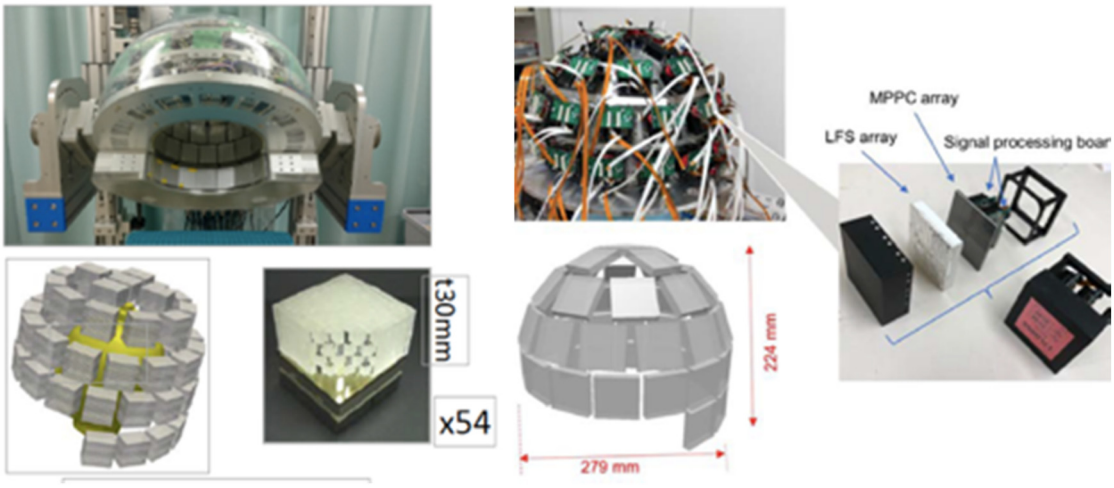

Figure 2: Example of the multi-modular design approximating the spherical shape produce many breaks in coverage, even when using intrinsically very compact SiPM technology. Examples shown from the Taiga Yamaya's group [48–50], at left with PSPMT-based modules, and at right with SiPM modules. The coverage improved with SiPMs (smaller gaps) but still many gaps remain.

reconstructed 3D images. The same group built the helmet style structure with three decreasing diameter rings of modules and with four additional modules placed at the top of the head. The executed structure has many angular breaks and is not optimal for sensitivity. The same observation one can make from the simulations by the AMPET team [51] team. Their design is also assuming a 3D shaped helmet. Interestingly, another group [52, 53] in their simulations have shown that a long cylinder placed low (and covering the eyes) can provide very similar sensitivity profile to the spherically shaped detector, except at the top of the brain.

But first, when designing these days dedicated brain PET, there is no more an option to separate sensitivity from resolution. The winning system of the next generation must be simultaneously outperforming the prior designs both in the achieved sensitivity and in the achieved spatial resolution parameters.

By this time (end of November 2021) after very vigorous developments of the last years in the dedicated brain PET scanners, with several novel instruments currently under construction, it becomes more obvious that new improved dedicated brain PET systems of the next generation are needed. In short summary to fully exploit the power of PET, the imagers need to better adapted to the imaging tasks, in addition to having improved parameters, like sensitivity and resolution (and also in the whole brain and not just in the brain center). Therefore, technical developments need to go in these diverse directions. Few examples are mobile PETs in ICU, surgery suit and epilepsy clinic, PET in proton therapy, but also upright PET optimized and ruggedized for imaging of the brain in motion. It is obvious that to benefit from the diagnostic power of PET no one-size-fits-all generic dedicated brain PET imager will suffice. We arrived to these conclusions after thorough review of the prior and new recently proposed art including the recent presentations and discussions at the BRAIN Initiative meetings and professional conferences such as IEEE NSS/MIC, SNMMI, EANM, APS, etc.

In addition, the economy of the scanners must be considered and addressed. To make an impact it must be possible to disseminate these high performing scanners after the development phase, that may indeed require high initial development costs. The recent example of the acute effects of the cost barrier **despite the revolutionary capabilities** of the new technology/devices, is the Total Body PET scanner. Here the cost is driven by the large volume of the expensive detector technology. Expensive even at the moderate level of ~3 mm FWHM or so spatial resolution, that is suboptimal for example in imaging of the brain, head/neck, prostate, etc. One can say with a high level of certainty that reaching the desired level of ~1 mm resolution in some imaging protocols is entirely out of reach for these scanners. Hence, pushing the solutions that provide high resolution, when needed (simultaneously with high sensitivity), and are economical is the direction that needs to be taken. As longer axial length and improved (smaller value) of TOF both give boosts to PET scanner's sensitivity, one can consider lower stopping power detector materials, much less expensive than fast crystal scintillators of the LSO family. Perfect and timely example is the fast plastic scintillator J-PET system developed in Cracow, Poland)

[54]. In addition to the Cherenkov radiator approach, this is the acutely needed development to continue with the Total Body Revolution, that despite the uEXPLORER, Biograph QUADRA, and UPenn Total Body PET is paused. The prompt Cherenkov radiation light option has the serious problem with very low light signal. The plastic option has so far limited spatial resolution (~4–5 mm FWHM) but a potential solution could be to use magnifying inserts [55–60] when high resolution, like in the brain) is necessary. In fact, the magnifying option is considered for the NeuroExplorer brain imaging project [61], to take the resolution down to the ~1 mm level in the specific areas of the brain such as cortex. It has to be emphasized that high resolution impacts sensitivity of detection of small structures due to the Partial Volume Effect [62–67]. So, both resolution and sensitivity improve at the same time.

Total Body PET scanner concept brings revolution to molecular imaging. The wealth of molecular/functional information provided by a single scan is overwhelming. Beyond the obvious issues how to store and analyze this vast amounts of data, and how to fuse the PET images from the almost 200 cm long Total Body PET imager with MRI images, the imaging scientists, as always, think about **improving spatiotemporal resolution** of the scanner. How to obtain better spatial and timing (Time of Flight, TOF) resolutions is always on their mind. Efforts to push timing resolution down to 50 ps and potentially even down to 10 ps were initiated. While attaining ~1 mm resolution in the Total Body imager is not immediately practically possible or even justifiable, due to other limiting factors such as large amount of recorded coincident events ("statistics") necessary to produce good quality ~1 mm resolution images in the human body and not just as before in the small animal body, it is possible to imagine now and plan to "attach" to the EXPLORER scanner a dedicated very high performing (~1 mm resolution, 100 ps or better TOF resolution and ~30–40% efficiency) compact brain imager (Figure 3).

This EXPLORER + Brain Tandem PET scanner may be closer to the ideal optimal human PET imager, providing there will be **little interference** between the two imager components (to image body and brain, respectively). Other options such as Torso Explorer plus Brain Imager are being discussed. Concerning only brain imaging, an exciting complementary idea is of a mobile high efficiency imager to image brain during upright natural motion, for example while walking on a treadmill. It fits into one of the key focuses of the Brain Initiative: "*Behaviorally active human neuroimaging that allows for movement in space during imaging in more natural environments while maintaining high resolution*". Sophisticated intelligent robotic support mechanics with very accurate motion correction are necessary in this very challenging case, to achieve high brain sensitivity in the whole brain volume, **while in motion**.

However, high-resolution imaging of the brain needs to and can be treated differently. In fact, the optimal solution here may be to use a *separate compact helmet style brain imager* operating in a tandem with the total body PET. Based on the solutions initially developed and implemented in small animal PET scanners, reconstructed spatial resolution approaching 1 mm seems to be possible.

The dedicated brain PET development trajectory over the last two decades was largely following the advances in the imaging technology (Figure 4).

The first generation of dedicated brain imagers was based on the standard vacuum photomultiplier (PMT) + crystal scintillator array technology but arranged in tighter rings surrounding the head of the patient. The second generation is using more compact position-sensitive vacuum PMTs and the latest variants are based on the solid-state Silicon Photomultiplier (SiPM) technology (Figures 5–7).

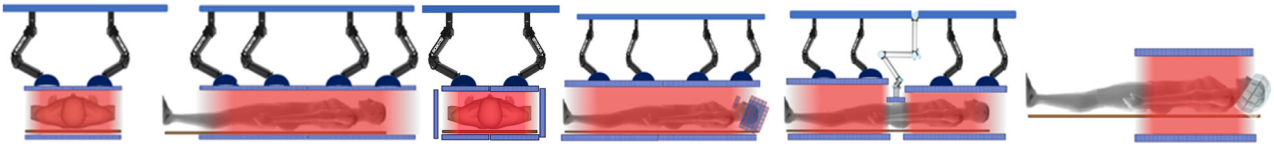

Figure 3: The potential long-term vision of the PET modality: the approach to the cost issue is to benefit from the TOF-delivered additional sensitivity through SNR (S/N) boost and to decrease the amount of (expensive) scintillator and readout, while maintaining key performance parameters at the same high level. The additional idea of adding high-resolution and high-sensitivity compact brain PET imager to the total-body-type PET imager is shown. Robotic arms may be used to support high-resolution magnifying inserts. Many implementation options can be considered with small-size technological insert/entrance ports, as well as in the gaps made temporarily in the system, as also shown, in the conceptual example for prostate imaging (second from right). To increase patient comfort, patients may use Virtual Reality glasses. Other shorter (torso +) long axial length designs with or without the dedicated brain imager and with or without robotic arms can be envisaged, as shown at right.

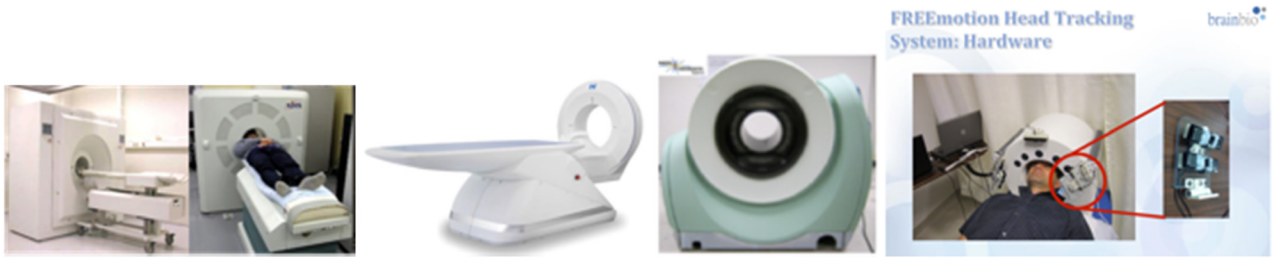

Figure 4: Previous generation dedicated horizontal PET brain imagers. Top from left to right: Siemens HRRT [67–69], jPET D4 [70] research system, Rainbow VHD from PINGSENG Healthcare Inc. [71], NeuroPET/CT imager from PhotoDiagnostic Systems [72, 73], and CerePET from Brain Biosciences [74]. First three imagers use standard vacuum PMT technology, CerePET is based on compact Position-Sensitive PMTs, and NeuroPET/CT is the only in this group based on silicon photomultipliers (SiPMs).

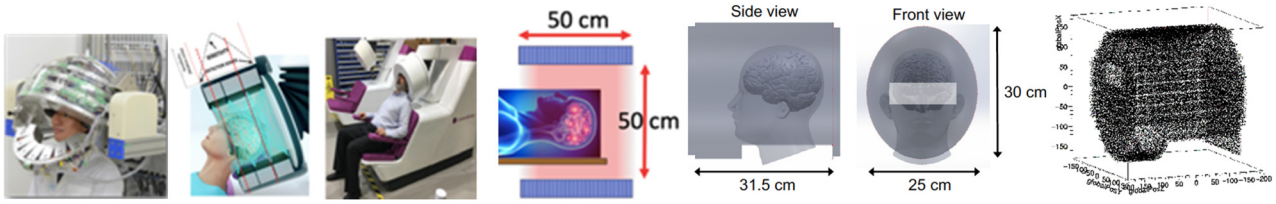

Figure 5: As an illustration, we show here several **examples of dedicated brain PET imagers.** First at left is a representative multi-modular design (from the many developed) by the Yamaya et al. group. Next is the short (15 cm axial coverage) CareMiBrain cylindrical 3-ring design from Oncovision [75, 76]. In the center is the sketch of the mini-Explorer-type scanner (such as NeuroExplorer [61]). This relatively large cylindrical design has about 50 cm axial length and 50 cm diameter, with improved 3D spatial resolution (smaller scintillator pixelation), good DOI and improved TOF timing, compared with the total body uExplorer design. The three drawings at right show CAD drawings of the very interesting helmet PET design from MGH [77] in the shape of an elliptical cylinder with front- and back panels. The front panel contains an eye opening and the back panel is hinged for easy patient access. GATE render of the implemented scanner showing detector module edges is shown at right.

Figure 6: Conceptual comparison of the three most relevant recently developed upright PET systems: CareMiBrain [47, 76], Positrigo [78], Prescient Imaging [79] Head has to stay still during scanning the brain in these systems.

Especially the MRI capability of the latest generation of solid-state-based photosensor technology (APDs and SiPMs) enabled designs of PET inserts in MRI scanners and many such systems were developed and new products are under development (example: MindView from Oncovision [82, 83]).

To illustrate what was developed so far either conceptually or to the level of a prototype, we selected examples of the dedicated brain PET scanners.

Discussion of the PET system parameters and implementation issues

The major issue with the implementation of PET imaging is that this extremely powerful molecular modality is expensive to use, and by this unavailable to many medical centers not only outside the developed countries but

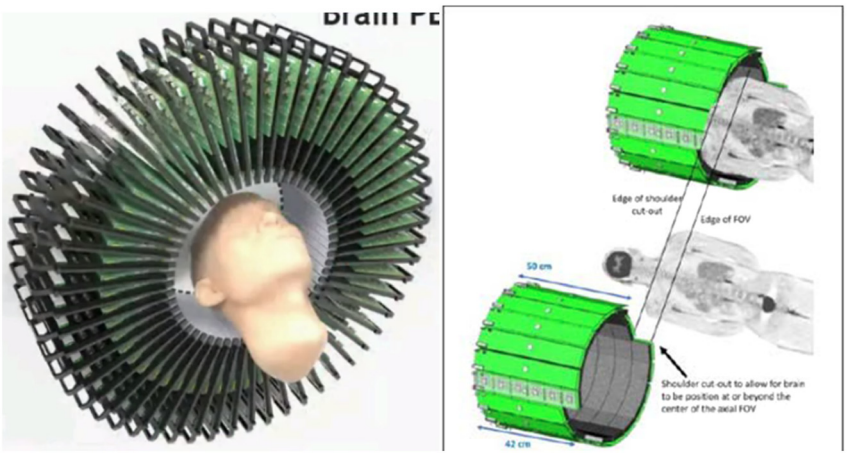

Figure 7: Two examples of the recently funded dedicated brain PET systems by the NIH Brain Initiative program. Left: SAVANT (Sherbrooke/MGH [80, 81]). Right: NeuroExplorer [61]. Both are pretty bulky and do not reach the limits of PET resolution. SAVANT is expected to achieve very high resolution (1.3 mm) in the central region of the brain only. NeuroExplorer has larger diameter ~50 cm and cutouts in the 6-th ring to accommodate the shoulders, allow for optimal brain positioning, and include carotids in the field of view.

actually in all countries. In addition, as discussed before, the generic whole-body PET scanners are not really well adapted to many imaging paradigms. Imaging of the brain is a very good example. At the other end, the imaging of the total body is not possible using standard technical solutions. uEXPLORER is an example. This 2 m axial length long unique revolutionary PET scanner was not adopted outside China. And even with the ~1 m long QUADRA imager from Siemens, there is still an issue of cost and therefore of the dissemination.

A possible solution to the above major dissemination issue, is to apply different technologies to the brain and to the rest of the body. In this optimal approach, we will benefit from the smaller diameter size of the brain imager that we need, compared with the rest of the body.

Therefore, the strategy could be to develop the very high-performance dedicated brain imagers coupled to the economical long axial length PET scanners. Brain imager should still be the best performance device. There is however always an issue of a rationale justifying these costs and challenges. In fact, in many imaging tasks, there is no need to push down to the 1 mm resolution level. Finally, the statistical argument is that the attainable resolution in many imaging protocols and tasks is limited by the event statistics (and the radiation safety imposed limits to the injected doses of the imaging agent) and even with the devices having extremely high intrinsic spatial resolution, that resolution cannot be benefited from and used in clinical practice. However, there is a potential for improvement here by implementing novel AI algorithms dealing with limited statistical data.

High sensitivity is primarily achieved via large angular coverage, high stopping power, and efficient background rejection before and during tomographic reconstruction (contributing to high Signal-to-Noise Ratio - SNR).

There is also a direct connection, between resolution and detection sensitivity in visualizing the small lesions or generally small structures, through the Partial Volume Effect – PVE. Time of Flight – **TOF** is providing sensitivity boost through the well-known SNR increase achieved by tighter TOF values in coincidence event acceptance criteria, in the process of tomographic reconstruction by rejecting more efficiently the background events (Figure 9).

Ideally, at about 10 ps FWHM (equivalent ~1.5 mm in space) there is no need for tomographic reconstruction [84], as the majority of the relevant background events are rejected by applying the tight timing coincidence window resulting in very good quality images [85]. Other, less ambitious and more practical in the near future, goals like 50 ps [86, 87], or 53.3 ps (equivalent ~8 mm in space (and suggested by Roger Lecomte, Sherbrooke].) TOF FWHM values were also recently suggested as the interim more realistic goals.

One of the many discussed at this time dedicated PET brain imager designs is a robust Top Hat PET structure composed of a cylinder and two flat panels: one at the top and one at the bottom, under the chin (Figure 8). Comparative geometric sensitivity of up to triple the sensitivity of the Biograph Vision [88, 89] and spatial resolution down to half of the Biograph Vision's resolution are predicted, depending on the details of the selected implementation such as stopping power, angular coverage, and pixelation (dead regions). **Sensitivity estimates up to 20%** and higher are being achieved in simulations, depending on the particular scanner design features.

Spatial resolution

Modern clinical PET scanners typically reach 3–4 mm FWHM resolution and that is too coarse a resolution for the

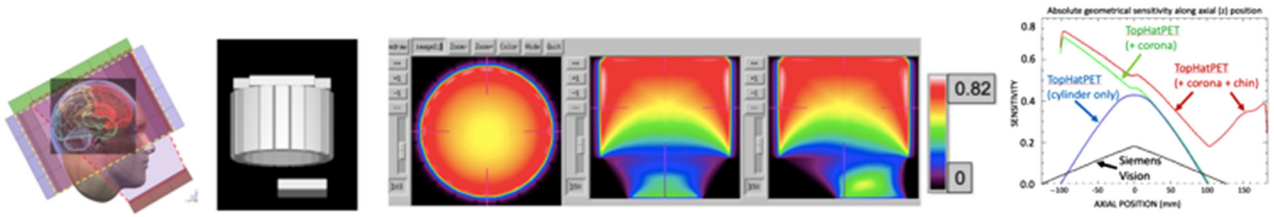

Figure 8: Graphical rendering of a simulated model for the Top Hat PET scanner. Center: three views (top, front, and side) of preliminary sensitivities with a color scale shown in the scale bar. The high importance of added top and bottom panels in increasing the sensitivity, especially at the top of the head where resides most of the brain is obvious from these calculations. The Top-Hat PET geometrical comparative simulations show that factor 2–3 in sensitivity increase compared with Biograph Vision is possible. (Simulations by Johan Nuyts, Loeven).

imaging tasks in many busy regions of the human brain, such as the primary motor and sensory cortexes. Also, the recent advances in studies on dementia require ever-improving spatial resolution of the imaging tools for example in imaging of the tau deposits to detect as early as possible the early signs of the disease.

Despite the almost two decades of development of the dedicated brain PET scanners, there is still an acute demand for higher performance. The desired optimal functionality includes not only much higher spatial resolution but also higher sensitivity through: (1) higher angular coverage of the brain; (2) higher detector stopping power; (3) and, if possible, additional sensitivity boost provided by the high Time of Flight (TOF) resolution. Surprisingly, the state-of-the-art of the dedicated brain PET has not yet progressed substantially beyond the Siemens' HRRT design, built already over 20 years ago.

Hence, there is a growing strong push to build the new generation of dedicated human brain PET systems that incorporate significant enabling technological advances in achievable sensitivity and effective spatial resolution. However, some of the reasons for lack of fast progress is

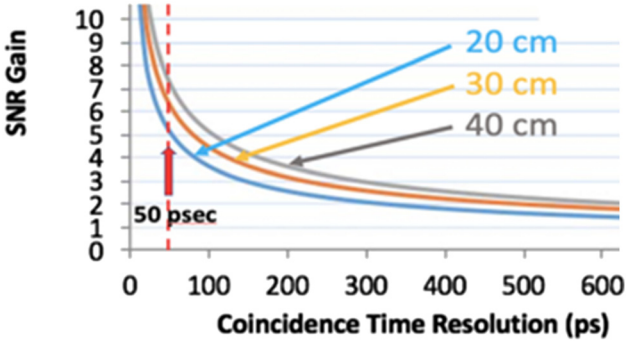

Figure 9: Sensitivity advantage provided by TOF. SNR improvement as compared with non-TOFPET system as a function of the time resolution for different diameters of the FOV with 20 cm being representative of the head [84].

that implementation of these novel technological features is expensive, especially if the universal full brain coverage imager needs to be equipped with the high volume and high granularity novel detector.

Very-high resolution, high-sensitivity "generic" dedicated PET brain imager that needs to be implemented with large numbers of small-size – high-resolution detector channels, requires also expensive electronics, large storage memory, and time-consuming data processing software algorithms. In some situations, supercomputer performance level is required. In contrast, if the very high-resolution (~1 mm) imaging were limited only to the task-specific selected regions, while keeping the rest of the volume at the still very high-performing 2–3 mm FWHM resolution, this would provide a remedy to the present practical obstacles. Therefore, we believe that a novel breakthrough solution is in limiting the resolution (and complexity and associated cost) of the imager only to the regions that require such increased performance in particular imaging tasks, as defined by the flexibly changing the imaging protocol.

In these novel compact designs, spatial resolution is maximized through small detector pixel sizes (high detector granularity) **down to ~1 mm or even less** in transversal sizes, with simultaneously achieved depth of interaction (DOI) resolution of down to 2 mm FWHM. The general concept here is to come as close as possible to the theoretical resolution limits in the 3D image reconstruction, that include positron range and a-collinearity effects. Minimizing the a-collinearity effect dictates compact helmet-type designs, as opposed for example to the barrel designs of the mini-Explorer type and definitely the standard clinical large diameter PET scanners. Performance close to 1 mm FWHM in the whole brain is predicted. (See also Addendum on spatial resolution toward the end of the article). Also, the "ultimate" achieved practically in the clinic spatial resolution may depend on how accurate is the motion correction of human subjects. Many motion correction approaches are investigated [90–95].

Impact of statistics. Very important and often forgotten element of the spatial resolution discussion is the impact of the statistical value of the detected signal, limited by the injected doses, biological uptake of the particular imaging agent, sensitivity of the system, and timing of the imaging scan (when done and for how long). To benefit from the ~1 mm range spatial resolution there has to be high enough number of the detected events during the scan to fill all the small 3D voxels in the reconstructed volumes, and per each time bin (if dynamic analysis is performed). Insufficient number of events in the image voxels results in very noisy images, that cannot be utilized unless software filtering adds controlled image blurring, which is in fact entirely negating the advantages of the very high intrinsic spatial resolution. This argument can be also formulated as that achievable statistics in fact sets the limit on the useful spatial resolution limit for the clinical imaging tasks, also depending on the imaging agent. High uptake of the specific imaging agents justifies the push for the best achievable detector performance, even if in the majority of cases the very high resolution will not be usable and the filtering of data, in the processing phase, as mentioned above, may be equivalent to using a system with moderate spatial resolution to start with. More sophisticated approaches such as denoising are studied to deal with limited statistics, that is especially important in low dose imaging.

How to achieve "super-high" spatial resolution

None of the so-far built or recently designed PET brain imagers achieves the resolution that PET technology promises, approaching 1 mm FWHM in the brain-size geometry (under 25 cm in diameter). The practical limiting issues range from technological to very high costs.

Indeed, a potential breakthrough in high-resolution PET brain imaging is to ***be able to visualize 1 mm structures in some key regions of the brain by implementing high-resolution inserts with as good as ~0.5 mm intrinsic resolution.*** Before such resolution was only achieved in imaging small animals. *This excellent spatial resolution could be achieved through a combination of (1) tighter PET geometry but primarily by (2) using a set of special adjunct ultra-high-resolution inserts with sub-mm (~0.5 mm) intrinsic resolution*. These compact insertable ultra-high-resolution PET **magnifying panels** could be flexibly and strategically placed next to the head and close to the particular regions of interest in the brain. Examples of such regions are primary motor and sensory cortexes (Figure 10).

The design and geometry of the inserts should be defined by performing very careful Monte Carlo simulations (Figures 11–14).

There is one important technical caveat with inserts, that to be able to install the inserts there must be enough space between the head and the inner surface of the imager. Hence, the very compact helmet-style scanners may be not applicable to this adaptation or conversion. On the other hand larger diameter systems such as family of total body imagers, and also the NeuroExplorer brain imager, as well as standard clinical PET scanners could be adapted to include inserts.

Brain PET detector design considerations

The imager of the next generation is envisaged as having up to tenfold increase in sensitivity by a combination of a tight yet expanded helmet style geometry, cutting edge TOF performance, high spatial resolution (impacting sensitivity of detection of small lesions through the Partial Volume Effect), and new generation of high performing dynamic/kinetic algorithms. For brain, PET imaging tasks whenever high spatial resolution is not necessary but only the pattern of the imaging agent's static and dynamic biodistribution with moderate spatial resolution (~5–8 mm) is required, initial estimates indicate that such an imager will be able to produce diagnostically useful data at dose levels **even *as low as 1 percent of the standard dose*.** For example, when imaging with 18F-FDG this will translate to about 100 μCi injected dose. The list of possible conditions where such a low dose system could be useful includes ***screening for dementia***, traumatic brain injury (TBI), depression, drug biodistributions, and other conditions where radiation exposure is an application barrier for the PET modality. Again, achieving the lowest dose operation would be only possible for tasks not requiring high spatial resolution, due to limited event statistics acquired al low injected doses. Also, low dose will conflict with requirements for dynamic analysis in addition to standard static imaging protocols, providing enough spatial voxel statistics.

With the high sensitivity being the main design goal, the preferred variant of the design will have relatively thick scintillator (25–30 mm of LYSO) to assure high stopping power. Important component of the high sensitivity

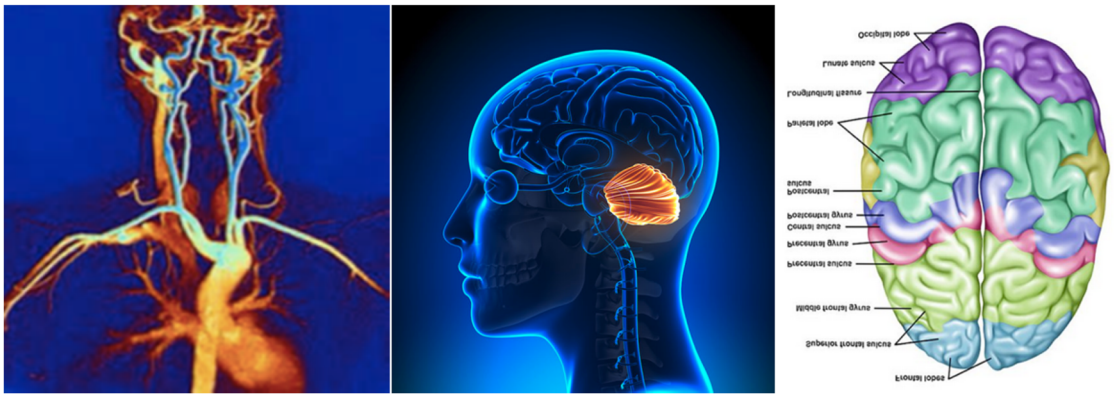

Figure 10: Examples of the desired magnification targets: carotids (to extract the cardiac input function needed for dynamic brain imaging), cortexes and cerebellum with the highest possible resolution ~1 mm: carotids. To extract cardiac input function for dynamic brain imaging, cortexes and cerebellum with the highest possible resolution ~1 mm.

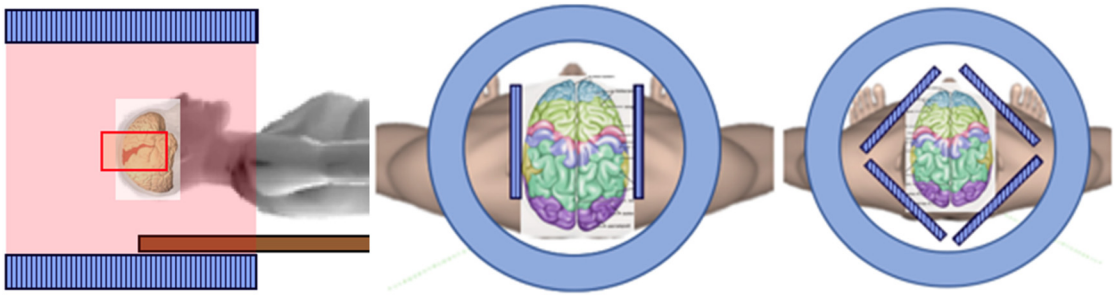

Figure 11: The concept of the magnifying inserts that could be used with the NeuroExplorer dedicated brain scanner to image selected brain regions.

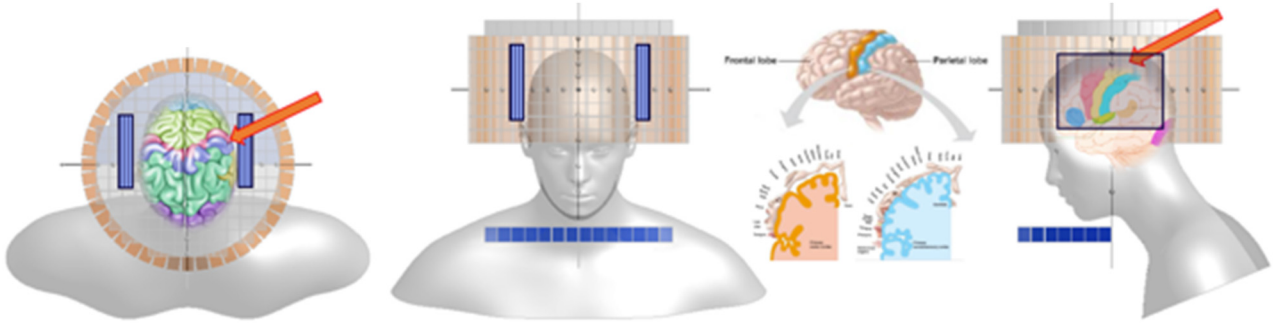

Figure 12: Another example of implementation of magnifying inserts used with a not too tight helmet-style scanner such as the top-hat variant shown here from UT Austin (original sketches kindly provided by Dr. Karol Lang).

performance in detection of small lesions is achieving high spatial resolution to boost efficiency of detection of small structures and lesions through the Partial Volume Effect [62–66]. High spatial resolution in a compact brain imager structure requires good Depth of Interaction (DOI) performance and good detector pixelation. Simulations show that DOI resolution as low as 2 mm is needed to achieve sub-2 mm spatial resolution in the whole brain volume. There are two major technical approaches how to achieve this level of spatial resolution, one is to use dual-sided pixelated scintillator arrays and the second is to use monolithic crystals, with one-sided or double-sided readout. Finally, TOF performance adds to the sensitivity calculation and it is better for the double-sided variant, either pixelated or monolithic. In addition, taking into account the naturally existing physical and optical gaps

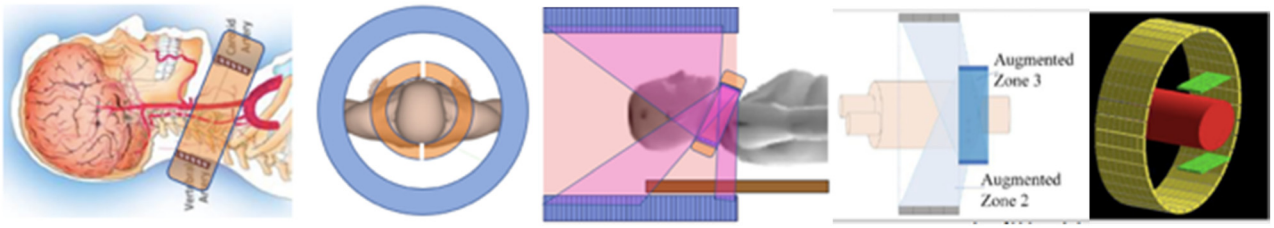

Figure 13: One possible conceptual solution for the input function monitor considered for the mini-Explorer-type brain PET such as Neuro-Explorer: ultra-high-resolution small ring assembled from two half-rings placed at left and right sides of the neck will provide large angular coverage with only few breaks, as compared with the "outsert" solution [56] as shown at right, with marked three separate groups of coincidence events. In the discussed, of a tight full-angle coverage geometry, the additional contribution of the mixed coincidence events will be much lower. Therefore, the carotids' imager can operate as a separate unit.

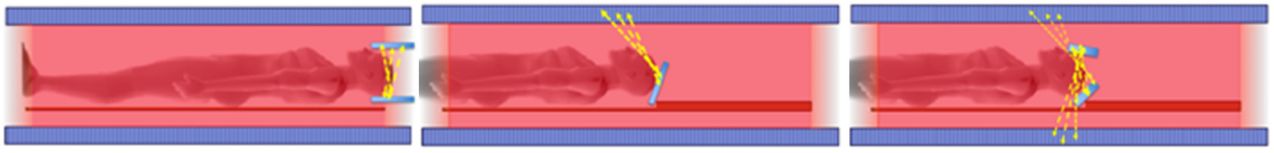

Figure 14: The very special case of imaging selected brain regions inside the Total Body PET scanner using magnification inserts. Artistic rough sketches showing ultra-high-resolution magnifying inserts in the total body PET scanner to provide truly high spatial resolution in the selected regions of the brain (as discussed before). The insert modules can either operate in coincidence between themselves or in coincidence with the close-by detector modules from the long cylinder of the total body PET. (Not up to scale).

between the individual detector modules, any design that minimizes these gaps will boost the sensitivity of the system.

Brain PET Detector Geometry Several groups performed simulations of compact brain imager structures. The results of recent simulations (already quoted Yamaya, AMPET, Schmidtlein, and Qiyu [96–99]) show that detector structures approximating a shape of a helmet with as spherical as possible angular coverage around the patient's head provide substantial increase, up to an order of magnitude, in the detection sensitivity in the brain volume. With the solid-state compact Silicon Photomultiplier technology, it is technically possible now to implement that design. Simulations show that close following of the shape of the human head is the best strategy to build high-performance brain PET. However, as mentioned, these simulations do not take into account the mechanical aspects associated with building such compact structures. In fact, close following of these prescriptions obtained from simulations is practically not feasible.

Specifically, the simulations by the Yamaya group show that instead of using a given number of detector surface elements in a cylindrical geometry one can rearrange these hypothetical modules in a hemispheric shape and substantially gain sensitivity especially at the top of the brain. While the cylinder can be well approximated in practice with the set of rings, the hemisphere is very difficult to cover with planar modules and many cracks will be left in between the modules. However, this could be possible if the detector surface could be shaped into a hemisphere.

The technology choices for the dedicated brain PET imager – interplay of parameters

As it often happens in the multi-parametrical space of the imaging detector technology, there are conflicts between some of the parameters, and balanced compromise in the selected parameter set has to be achieved, not only based on the performance to be achieved but also on practical aspects such as complexity and cost. Improvement of TOF performance became recently one of the key competitive efforts in the imaging community and in industry. Every 50 ps improvement is hailed as an important advance over competing approaches. However, careful review of the dependence of the S/N ratio for a 20 cm head-like object shows that the improvement is actually small and it is often off-set by technical choices that have to be made to achieve that new record levels of timing resolution. Such as pixel size and DOI resolution (impacting spatial resolution), scintillator thickness (impacting annihilation

photons stopping power and DOI error), and finally geometry and angular coverage. In addition, complexity and sensitivity (temperature dependence, etc.) of the system and its bulkiness, cable burden, and finally cost are increased in the cutting edge TOF capable systems.

In fact, due to the bulkiness of the present-day PET TOF capable modules, it is not possible to build a tight module array structure covering head in 3D. Instead the investigated helmet type systems (Yamaya et al.,) have many breaks in coverage and the associated sensitivity loss is not negligible.

The initial theoretical predictions [100, 101] are that implementing best practices like dual-sided fast scintillator readout with SiPM arrays can take the resolution down to about 100 ps FWHM level at best and not much beyond, even when benefiting from the Cherenkov prompt light component. The same analyses predict that real TOF advantage will become possible when the next frontier of 10 ps or so in time resolution is reached. However, this will require the annihilation photon detection technique to be based on a different physical principle, or by using new super bright and fast scintillators, etc. but none of these developments is expected to be soon available.

The future dedicated brain PET scanner must be able to operate in a **dynamic mode** to provide kinetic model analyses and parametric images. Therefore, the image-derived (cardiac) input function (IDIF) must be provided. The leading two implementation options are: (1) extraction of the signal from the carotids (i.e., carotids have to be in the field of view of the ~1 mm resolution scanner); or (2) implementation of another separate companion or adjunct IDIF detector, extracting the input function either from the aortas, or the wrist or the ankle.

Finally, ultra-high imaging resolution cannot be realized without effective **motion correction**. New techniques are being developed based on face features imaging, that allow to achieve 0.2 mm resolutions.

On a practical side, an absolute requirement, is the **system's stability** outside the laboratory environment, and the critical ability to perform **robust repetitive calibrations in the clinical environment**, for example under varying temperature conditions. Some (actually many) candidates for the high performing systems are not easy or not even possible to calibrate outside of the well-controlled laboratory environment (requiring special additional phantoms, radioactive sources, opening the detector geometry that is naturally tight during clinical operation, and requiring additional computing power to perform these calibrations, etc.) even when using different sophisticated AI tools, such as machine learning, neural networks, etc. And these still novel and not fully understood AI tools have to be properly used, or otherwise they may create issues in image reconstruction. Proposing the AI software tools does not yet automatically solve all of the above calibration issues.

In our opinion, the dual-sided readout is optimal for the next-generation high-end general use dedicated brain PET systems. It is the only design that minimizes the edge and non-uniformity effects in the detector modules, and has a regular structure of the detector elements that produce regular patterns in the flood images used in calibrations and thus permitting clear spatial separation of the 3D detector pixels with no overlaps with close tight positions in the images and with robust depth identification formulas used both to extract DOI positions and to correct for TOF variation with depth of interaction. In these dual-sided designs, TOF is also improved due to the ability to correct for difference in scintillation time propagation in the crystals by defining the position (DOI) of each event, and this consequently provides the sensitivity boost, as mentioned before (proportionally to the inverse of the TOF resolution). The variety of the single-sided DOI readouts, with some examples shown in the figure below, all show difficulty in achieving the **uniformity of response**, in some cases having also modular edge effects, and therefore presenting serious calibration challenges.

TOF panels approach

Another, very different from helmet-type approach, is to fully benefit from the best possible TOF performance (predicted to be of the order of 50–70 ps FWHM [86] allowing to partially compensate for the cut in the physical stopping power as the result of decreasing scintillator thickness (as the measure to lower costs). DOI resolution is then equivalent to the scintillator thickness of 3–5 etc. mm. TOF resolution is maximized in this robust one-sided readout design by physically removing the depth variation. Imaging PET scanners of this type could be implemented wherever there are requirements for compactness, mobility, open flexible geometry, upright geometry, economy, etc. One of the discussed recently approaches is to use 30 cm square TOF PET panels with 5–10 mm-thick scintillator. This will allow for flexible open geometry economical mobile designs [86] (Figures 15 and 16).

Therefore, benefiting from the high-resolution TOF performance enabling open flexible imaging geometry, one of the novel key attractive features is configurational flexibility. Inclusive of many possible PET imaging configurations. Used also in mobile bedside systems. In ER and ICU, surgical suit, and epilepsy clinic, or assisting with

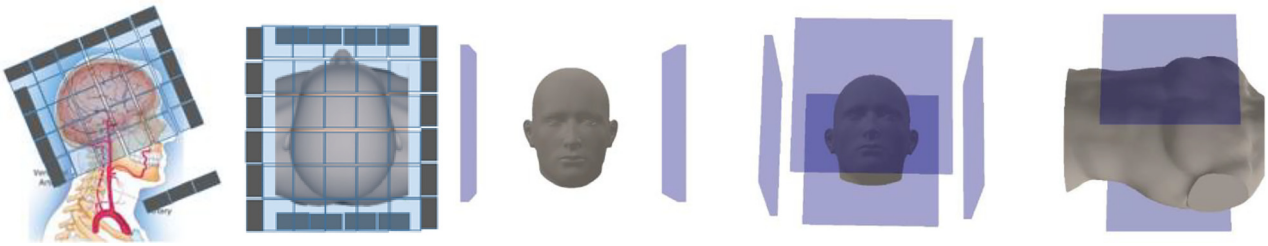

Figure 15: Examples of the TOF PET multi-panel flexible geometries. Flat panels made with tightly arranged ~5 cm square modules with 5 mm thick LSO arrays. Left: a half-size panel used under the chin to extract the input function signal from the carotids. Right: Two-panel (center) and four-panel (at right) detector placement when imaging the XCAT head phantom and the two-panel detector placement for XCAT torso phantom imaging (right) that could be also used in extracting aortic input function for dynamic brain imaging.

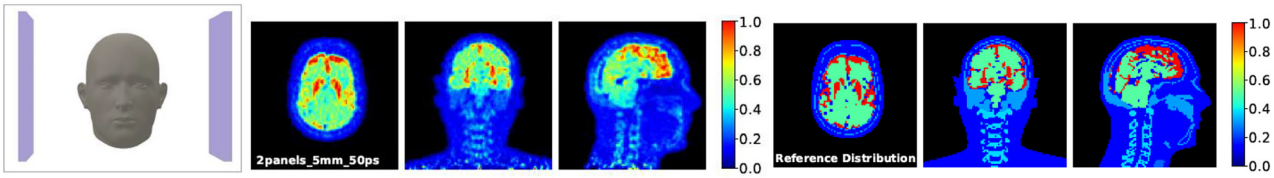

Figure 16: Example of the quality of reconstructed images of the digital XCAT phantom of the head and neck region using **only two detector panel** (maximum open geometry). The images were normalized with the total activity within the head mask and scaled with the max voxel value in the true - reference images shown at right [From 86].

radiation therapy delivery, such as proton therapy, brachytherapy, and focused ultrasound therapy. In addition, hybrid imaging systems can be proposed combining for example EEG and PET (Figure 17).

And also imaging brain in natural situations such as walking on the treadmill. Or during upright meditation. During these imaging tasks, the optimal multi-task PET system needs to offer flexibility while maintaining high performance. In order to be able to optimize angular coverage in varied brain imaging tasks, and to achieve the best TOF values, while maintaining high mobility and structure flexibility, a system of TOFPET flat panels, ultimately mounted on individual robotic arms, could be optimal. In fact, several groups discussed using planar TOFPET modules (another example: [102, 103]). Such a modular system can naturally be expanded from brain/head to imaging torso and then the total body. The configurational flexibility can be increased by using robotic arms, to make it even more readily adaptable to many different brain imaging paradigms.

Magnetic resonance imaging (MRI) compatibility and PET inserts in MRI

Ideally some systems could operate as a simultaneous PET/MR device with PET being inserted into the MRI bore [104–109] (Figure 18).

Figure 17: Two robust open flexible geometry concepts shown at left using two or four planar TOFPET panels mounted on precision robotic arms of the moving gantry, to secure safe and accurate flexible positioning of the panels, both specific to the patient and to the imaging task, for example, in surgery or when measuring the stimulation of deep regions of the brain by inserted electrodes. The modules can be placed to avoid or minimize mechanical or space conflicts that are not possible with the standard fixed size designs of the PET scanners. The flexibility of design can go even farther. As each of the TOFPET panels is actually an array of TOFPET modules, the design can be further split into smaller units, to better adapt with the busy area around the patient's head. At right is shown an example of the subject wearing the VR glasses and walking on an omnidirectional treadmill. Two TOFPET panels mounted on the robotic arms are shown scanning the brain here.

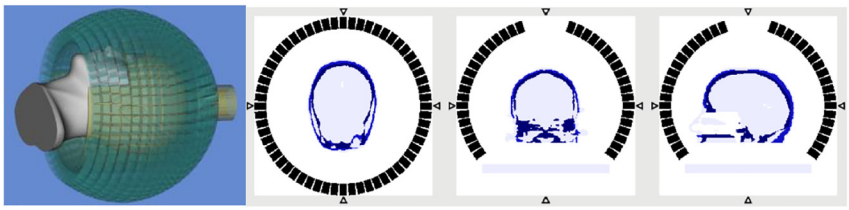

Figure 18: Example of the PET insert geometry being developed for the 7 T MRI scanner. Left: spherical geometry scanner. Right: Scheme of the simulated Zubal phantom with the scanner.

However, the requirements of full compatibility and primarily not having any adverse effects on MRI operation from the PET insert, are severely conflicting with the task of optimization the PET component. Therefore, following the recent example of the Flexible PET system from Shimadzu [110], one can develop PET imager that can be used sequentially with MRI, using the same prone patient position in both modalities, and will allow to decouple the PET optimization from the restrictions imposed by the above compatibility including fitting the RF coil sizes etc. In this case, the PET scanner would operate just outside the MRI magnet bore, and without impacting the MRI operation.

The critical challenge of not interfering with the operation of the MRI scanner, is posing severe restrictions on the PET device geometry (not only the mechanical fit but also interplay with the MRI RF coils) choice of materials in the PET detector and shielding against electromagnetic interactions, that also impact PET operation (background noise in the signals). This very challenging technical subject was covered before in many papers, and we will not cover it in this report. However, to illustrate the recent progress, we will only use here two recent examples of PET inserts: a cylindrical MINDView system, and the MGH insert under development for the 7T Siemens MRI, that is also a very interesting spherically shaped structure [108, 109].

Mobile, wearable PET

Special category of the brain scanners is the **motion tolerant variety**, that follow the limited motions of the head either by being attached to the head and/or by active motion correcting mechanics, such as robotic arms (Figure 19, Table 1).

The pilot pre-clinical development effort was in the RatCap [111] wearable awake rat PET scanner, attached to the rat's head (developed at the Brookhaven National Laboratory, and now produced by SynchroPET). Latest variants of the proposed human compact systems are the wearable compact lightweight helmets, also with the assistance of active mechanical support, such as using safe robotic arms (Youngho Seo, UCSF et al., proposal submitted for funding to the Brain Initiative NIH).

The revolutionary concept of a wearable brain PET [96–99, 112–117] as the new unique imaging tool to assess brain activity during realistic tasks (like "walk in the park", social interaction, standing or walking, etc.) has many challenges preventing it from being fully or even optimally implemented. There is a contradiction between the requirements of compactness, lightweight wearability with freedom of motion on one side, and high operational performance (specifically sensitivity) on the other. High-performance imager is bulky, heavy, and wearing it presents a safety hazard. TOF electronics is complicated,

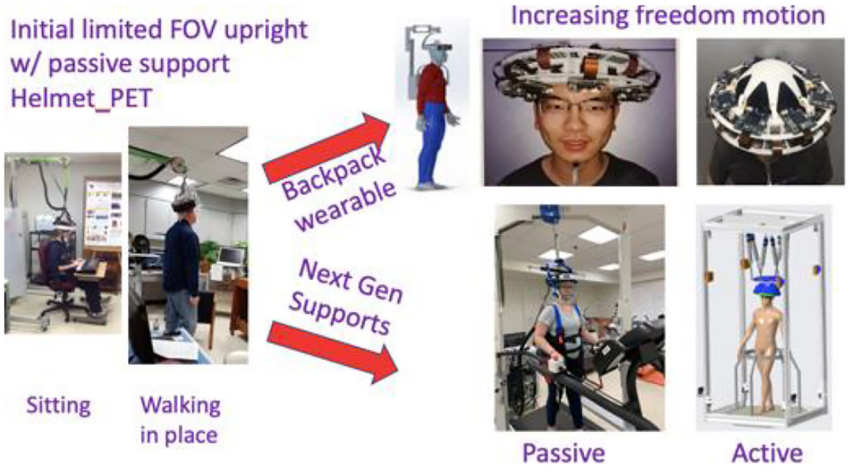

Figure 19: Two separate trajectories of development of the motion tolerant upright imagers. Wearable backpack supported system provides maximum motion tolerance at the expense of sensitivity Implementation of intelligent robotic supports may indeed solve the issue of the limited axial coverage and poor sensitivity of the first generation of wearable brain PET systems.

Table 1: Some expected features of the next-generation mobile brain imager.

– Upright/reclined/horizontal mechanical options
– ~1 mm PET resolution in the whole brain volume (1.5 mm pixels/3 mm DOI)
– Sub-mm resolution in the carotids to extract Cardiac Input Function for dynamic brain imaging;
– Ultrasound guidance for precise positioning and motion correction of both carotids;
– Est. 150–300 ps TOF resolution
– Over 20% sensitivity (i.e., about 2× Biograph Vision)
– Passive/active (f.e. robotic arms) safe support mechanics following limited head motions with rotations while bearing the major part of the weight
– Optical multi-camera motion correction system with 0.2–0.5 mm accuracy
– Kinetic multi-tracer algorithms
– AI analysis enhancement
– Dual modality option PET/EEG

bulky, and generates heat requiring active cooling, more bulky and heavy electronics, increased cable burden, etc. But the key limiting factor is the stopping power of the radiation sensor dependent on the amount and weight of the heavy scintillator material. Any wearable scheme must recognize this fact and the imposed limitation. Unlike in cancer diagnostics, low sensitivity (translating into high dose) is adverse to many applications where radiation dose is an issue, such as research on healthy subjects and screening tests for many conditions, such as dementia, depression, mild Traumatic Brain Injury (mTBI) in sports, stroke, etc.

We believe that potentially the only practical solution to this conflict of sensitivity vs mobility is to develop a system that will recreate realistic environment using high performance mobile head following detectors. One can for example implement: (1) intelligent robotic and safe mechanical support; (2) creating realistic VR environment simulating with high accuracy the conditions of the real world and immersive experience, with walking, navigating, talking to others, etc. The new "natural" environment could be highly physically compressed in space by using 1D and 2D treadmills and/or small walking space, that will limit the challenge both purely mechanical and functional but also from a critical safety point of view. Instead of the "walk in the park" this will be a "walk in the VR space". Here, the new challenge will be how to closely simulate and model the real environment and experience of the subjects. While in principle the lightweight system's weight could be supported by passive systems and even worn by the subjects with a backpack style support, they will not address sufficiently the *critical issue of safety*. We believe that only the intelligent support system with active support equipped with feedback and monitoring of motion progress and activating special automatic protective measures and quick decoupling/relief of the imager from the subject will minimize the safety concerns. Also, such a system will be equipped with the safety harness that will prevent subject from falling due to tripping, tiredness, etc.

Novel concepts

Cherenkov radiation in fast timing PET

In addition to continuously improving operation of fast scintillators with fast photodetectors and fast readout (fast amplifiers and ASICs etc.), and the development of the new materials to reach the still far-distant very ambitious goal of 10 ps FWHM in PET, several groups are setting the intermediate goals from ~60 to 30 ps and demonstrate in simulations and in preliminary experiments the strong advantages of these relatively moderate TOF values in system operation. The most impressive results come from the Miro-channel Plate (MCP) PMT-based detectors where the Cherenkov radiator replaces the standard PMT window and is directly coupled to the photocathode of the MCP. In the recent study using two MCP PMT modules with lead glass windows doubling as radiators, 32 ps FWHM was obtained [17]. Most importantly, the authors have demonstrated that they can produce good quality images of the phantoms without using standard 3D reconstruction software but just from direct axial position (between the detectors) calculation from TOF differences, defined with the axial accuracy of 4.8 mm (corresponding to 32 ps FWHM). The authors show that this performance is sufficient to produce cross-sectional images of a positron-emitting radionuclide directly from the detected coincident annihilation photons, without using any tomographic reconstruction algorithm. Next, the same group will investigate MCP windows made from the BGO scintillator, that will operate as the (slow) scintillator with added very fast Cherenkov signal produced in the BGO plate. However, this technology is still in the very early development stages, limited to very small detector sizes and thin radiators, and with large dead spaces if used in an array configuration, and consequently suffering from low sensitivity. However, brain imaging can become again one of the first human system implementations on a path to larger PET systems ultimately including the total body imagers.

Multi-gamma imaging

It is highly desirable to be able to simultaneously image two or more brain imaging agents. For example, in imaging of drug addiction. Nora Volkow from NIH requested such imaging ability during the recent Brain Initiative meeting [118, 119]. Also, in theranostics applications different imaging agents could be used to better assess the treatment. The limitation of PET is that all positron emitters produce the same 511 keV annihilation photons and one needs to look at the signal dynamics to deconvolve the contributions from different imaging agents. A potential solution is to use multi-gamma emitters that in addition to positrons (with accompanying annihilation photons) emit other characteristic gamma rays. In general, a combination of PET, SPECT (with their signature gammas) and Compton events could provide the additional identifying information to separate the signals from different imaging agents used in the mixture. Several multi-gamma approaches were recently proposed by the Yamaya [120–122] and Moskal [123] groups. The Yamaya group introduced the Whole Gamma Imaging (WGI) concept and demonstrated it recently in a small animal prototype system (Figure 20).

The hybrid method successfully combined PET and Compton events to enhance image quality. They experimentally demonstrated using 89Zr as positron/gamma emitter that image contrast was improved while noise was suppressed. Their plan includes the hybrid reconstruction further combining 511 keV Compton events and imaging tests with radionuclides other than 89Zr.

J-PET and positronium concepts. Exploiting positronium information

Compared with crystal-based PET detectors, J-PET built of plastic scintillators provides superior time resolution, lower pile-ups, and opportunity of determining photon's polarization through the registration of primary and secondary Compton scatter events in the same detector [124, 125].

Recently, the characteristics of the total body (TB)-J-PET were estimated by simulation following the NEMA NU-2-2018 protocol utilizing the GATE package [54]. The simulated detector consisted of 24 modules, each built out of 32 plastic scintillator strips (each with cross section of 6 mm times 30 mm and length of 140 or 200 cm) arranged in two layers in regular 24-sided polygon circumscribing a circle with the diameter of 78.6 cm. For the TB-J-PET with an **axial field-of-view (AFOV) of 200 cm**, a spatial resolutions (SRs) of **3.7 mm** (transversal) and **4.9 mm** (axial) were achieved. The values of scatter fraction and spatial resolution obtained in these pilot simulations are comparable to those obtained for the state-of-the-art clinical PET scanners and the first total-body tomographs: uEXPLORER, PennPET, and Siemens QUADRA. The time-of-flight resolution for the TB-J-PET is expected to be at the level of CRT = 240 ps FWHM. Interestingly, using the same detector principle, a shorter J-PET with an AFOV of 75–100 cm, could serve as the economical high-performance brain imager (Figure 21).

This idea warrants a careful study if indeed optimizing the design for brain/head/neck could result in a clinically valid system.

In addition, the authors propose the novel method of positronium imaging of the human body [126]. Positrons injected into the human body create in more than 40% cases the bound state of electron and positron, the positronium atom [127]. Currently, in the PET technique, the phenomenon of positronium production is neither recorded nor used for imaging. They discuss that properties of positronium atoms such as production probability and life time depended on the environment, as well as 3γ to 2γ rate ratio which can be obtained during a routine PET imaging, may deliver information useful for the *in vivo* cancer diagnosis and grading [128, 129]. The authors hope that in the not so distant future such information will become available first in research and then in clinical practice.

The key concept is that during the positron emission tomography about 40% of positron annihilations occur through the creation of positronium which may be trapped within and between tissue molecules. Positronium decays in the patient body are sensitive to the nanostructure and metabolism of the tissue. This potentially powerful diagnostic property is not used in the present PET systems, while it is in principle possible to use the modifying effect of the micro-environment on the properties of positronium

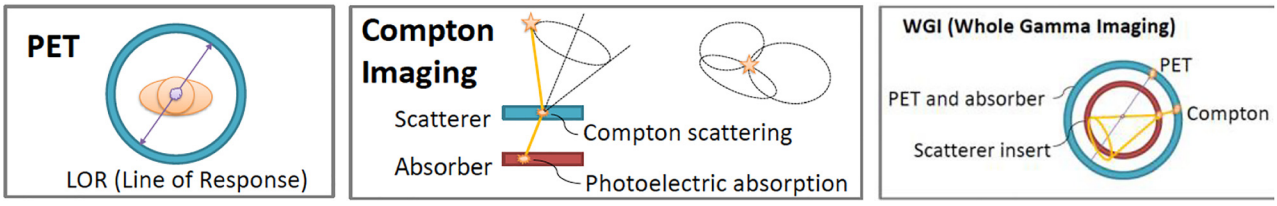

Figure 20: Whole Gamma Imaging (WGI) term introduced by the Yamaya et al. group is a mixture of PET and Compton [120–122].

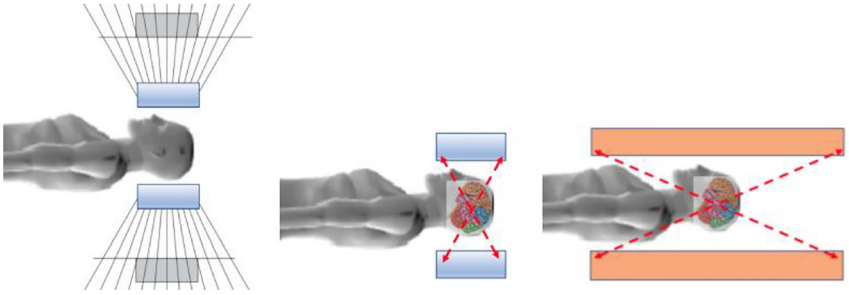

Figure 21: Illustration (not-to-scale) of the large angular coverage differences between the standard-sized PET detectors (~25 cm axial length) placed at about the standard distance from the head during head imaging protocols in the clinical PET scanner (presented as gray boxes at left) vs the most compact geometry (blue boxes) and the ~0.75–1 m long axial length scanner when used in brain imaging (orange boxes). This angular coverage factor translates into substantial sensitivity boost.

as additional diagnostic biomarkers for cancer, also during therapy. Pilot *in vitro* studies show differences of positronium production probability and of the mean half-life between the healthy and cancerous tissues, hence indicating that these differing properties may potentially be used as *in vivo* cancer indicators in patients [128, 130]. A method is being developed by the authors of positronium lifetime imaging in which the lifetime and position of positronium atoms are determined on an event-by-event basis. For the method to be useful, application of β+ decaying isotopes emitting prompt gammas (e.g., 44Sc) are needed. The time and position of positronium annihilation from the back-to-back 511 keV photons originating from the interaction of positronium with the surrounding atoms and bio-active molecules needs to be measured. The accompanying prompt gamma is used for the determination of the time of the formation of positronium. The authors estimate that with the large angular coverage of the long axial length total-body PET scanner, the sensitivity of the positronium lifetime imaging, requiring coincident registration of the back-to-back annihilation photons and the prompt gamma, is comparable to the sensitivities of the standard PET scanners [123] This concept benefits from the differences in the angular distribution of the emitted 511 depending on the type of tissue. This adds additional diagnostic power to the standard PET modality. The authors propose the novel method of positronium imaging of the human body. Positrons injected into the human body create in more than 40% cases the bound state of electron and positron, the positronium atom. Currently, in the PET technique, the phenomenon of positronium production is neither recorded nor used for imaging. They discuss that properties of positronium atoms such as production probability and life time depended on the environment, as well as 3γ to 2γ rate ratio which can be obtained during a routine PET imaging, may deliver information useful for the *in vivo* cancer diagnosis and grading [123, 131]. The hope is that in the not-so-distant future such information will become available, first in research and then in clinical practice. As discussed before, the assumption is that these concepts will be transported also to imaging of the brain.

However, as also discussed, and not only in the case of J-PET, with much more emphasis on (and need of) high spatial resolution approaching 1 mm in the brain, the optimal system may have: (1) the major component that is the total body (a.k.a. long axial length) dynamic multi-organ imaging system with moderate spatial resolution; (2) brain imager as a separate high-sensitivity and high-resolution scanner; and (3) a set of ultra-high-resolution inserts that would operate in a magnification mode with the detectors in the main detector, as shown in sketches above. In fact, brain imaging could be also done with magnifying inserts, but it would be suboptimal, especially in imaging the deep brain structures. Still it may be an economical good performing solution. In that simplest variant, the PET system of the future may have total body length coverage using robust economical technology solution like used in J-PET, appended with a set of selected magnifying inserts. While challenging from the reconstruction algorithms' and calibration point of view, this may be is the acutely needed balanced solution between the functionality, performance, and cost to push forward.

Summary

We are still on a development path and there is still a lot to be done in order to develop optimal brain imagers. Optimized for particular imaging tasks and protocols, and also mobile, that can be used outside the PET center, in addition to the expected improvements in sensitivity and resolution. To be more efficient, flexible, adaptable designs are

preferred. This task is facilitated by improving TOF performance that allows for more open adjustable limited angular coverage geometries without creating image artifacts. As achieving uniform very high resolution in the whole body is not practical (including prohibitive costs) the total body + brain schemes like the ones discussed above with the J-PET example, should be actively investigated. Indeed, it may be the pragmatic choice when having further dissemination of the PET modality in mind and especially the accelerated acceptance of the total body concept, in research but then in clinical practice. And brain imaging of the next generation is an important part of that discussion.

Acknowledgments: The author is thankful to Professors Pawel Moskalik and Ewa Stępień for their invitation to contribute to this special edition of the journal to cover the PET brain imaging but the author wanted also to emphasize the common aspects of the next-generation PET imagers, that bring to focus the necessary pragmatic approaches like the J-PET concept.
Research funding: None declared.
Author contributions: All authors have accepted responsibility for the entire content of this manuscript and approved its submission.
Competing interests: Authors state no conflict of interest.

Addendum 1: Limits of spatial resolution in PET

The basic idea of the next-generation PET systems is to take the spatial resolution of the system to its limit imposed by the physics of the PET process, the motion correction accuracy, and the statistical event limitations in creating high-resolution images composed of many small 3D pixels with high enough event statistics in each pixel to produce "good quality" images. The key physical contributing factors are: positron range and a-collinearity between the emission directions of the two 511 keV annihilation photons (Figure 22).

In addition, one needs to minimize the detector contribution by its proper design. In technical terms, it means to implement: (1) smallest possible physical size of the system, limiting the maximal distances between the opposed coincident radiation sensors detecting the two 511 keV annihilation photons from the coincidence pairs, and (2) high intrinsic spatial resolution of the detector modules, including the depth-of-interaction (DOI) measurement. And DOI resolution is especially important in compact systems.

Using the approximate theoretical formulas one can get an estimate that sub-mm resolution for a brain-sized or breast-sized imagers is possible. In addition, there is **experimental evidence** that implementing the above optimization strategy works in several successful implementations in small animal PET scanners, such as PawPET and few other [examples: 132–134]. In these implementations, still not yet fully perfected, the reconstructed spatial resolution of 0.5–0.7 mm FWHM was achieved using F-18-based imaging agents.

Many papers dealt in the past with spatial resolution limits of the PET detectors [Example: 135]. An example of the empirical formula for the spatial resolution limit for a pixelated PET detector is:

$$FWHM = 1.25\sqrt{(d/2)^2 + b^2(0.0022\,D)^2 + r^2 + p},$$

where d is width of the pixel, D is the distance between the opposed coincidence detector modules in the contribution term expressing the a-collinearity of the two coincident annihilation photons, r is the positron range, and b is the blurring effect due to motion and the last term is due to parallax effect (p). 1.25 is the empirical factor related to the degradation of the point spread function (PSF) due to the non-uniform sampling of the LOR in the FOV and the image

Positron Range in Water

Nuclide	Max (mm)	Mean (mm)
^{11}C	4.1	1.1
^{13}N	5.1	1.5
^{15}O	7.3	2.5
^{18}F	2.4	0.6

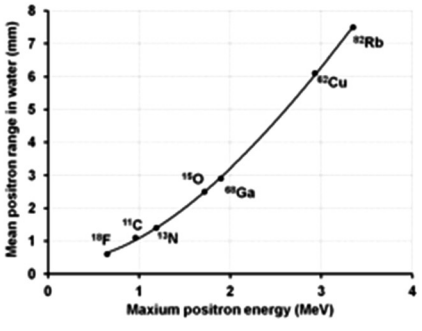

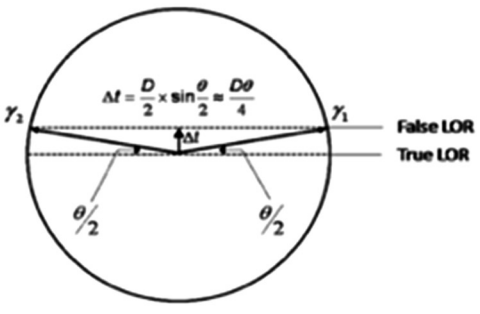

Figure 22: Left and center: The positron range for several positron labels. Right: a-collinearity between the two 511 keV annihilation photons emitted back-to-back introduces error in position definition of the annihilation point, that increases with the diameter/size of the detector.

reconstruction process. This value is estimated assuming an analytical reconstruction algorithm such as the filtered back projection (FBP). From the formula, there are several key contributions to the reconstructed spatial resolution: physical processes (positron range and a-collinearity of the two annihilation photons), detector defined pixelation and DOI resolution, and also ***motion-induced error***.

From the formula, an improvement can be achieved by making a more compact detector, using smaller-sized detector pixels, lowering the parallax effect, and avoiding blurring due to the motion. As formula provides, error due to the a-collinearity of the two annihilation photons increases with the distance between the modules. Therefore, closer structures are preferred, also from the sensitivity point of view, as well as due to smaller size, lower weight and reduced cost.

Below are shown two examples of the predictions from the above formula:

(1) for a 25 cm diameter (tight brain size) detector and F18, 2 mm transversal detector resolution pixel size, and ***assuming no blurring due to motion or parallax effects***, the resolution limit is 1.75 mm FWHM.
(2) as in (1) but for 1 mm intrinsic detector resolution pixel this limit value changes to 1.19 mm FWHM.

In the paper by Shibuya et all, the authors calculated the non-collinearity contribution only: "For example, the limit of PET spatial resolution are calculated to be 0.5 mm for a 10-cm diameter scanner, 1.2 mm for a 40-cm diameter scanner, and 2.1 mm for an 80-cm diameter scanner." These results are consistent with the formula we use above. To achieve better resolution than formula predicts, modeling of the positron range and of the a-collinearity is expected to provide some improvement.

DOI contribution. The need for good DOI resolution is illustrated in the plots below showing calculated radial spatial resolution for several LSO crystal thickness designs (source: Johan Nuyts, Lowen, Belgium) (Figure 23).

In this compact brain scanner example, the inner diameter of 25 cm and **3 mm and 1.5 mm** scintillation pixel sizes were assumed. DOI resolution in the 1–7 mm range was assumed. To maintain ~1.5–2.00 mm resolution in the whole brain volume in such a tight detector structure, DOI resolution should be 2–3 mm. Many studies investigated how to achieve good DOI resolution [examples: 136–138].

In addition, it is important to take into account other contributing practical limiting to the usable spatial resolution, that are often underestimated, and are related to the brain position recording and motion correction through the duration of the scan, and the ability to apply these accurate time sensitive corrections to the recorded data stream, before the image reconstruction process. Patient comfort is an important contributing factor, especially during long scans during dynamic brain imaging sessions. It is critical in order for the high-resolution imaging protocols to be successful, to develop a robust, concurrent or complementary and yet partially overlapping motion correction system that can be used in different imaging situations. There is a lot of experimental evidence that excellent intrinsic spatial resolution cannot be realized as readily in clinical environment, unlike in the controlled phantom studies, if there is inadequate human motion correction.

A very important and often forgotten element of the spatial resolution discussion is the impact of the statistical power of the detected signal, limited by the injected doses, biological uptake of the particular imaging agent,

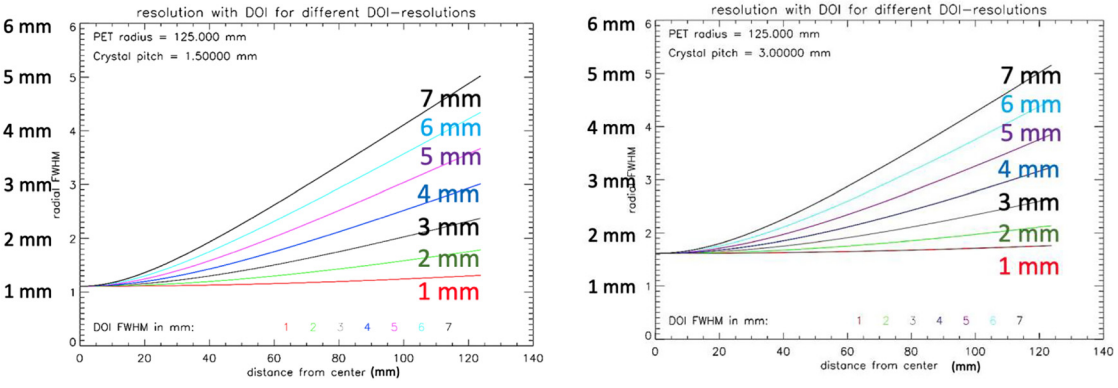

Figure 23: The need for good DOI resolution is illustrated in these plots showing calculated radial spatial resolution for several DOI values (private communication: Johan Nuyts, Loewen, Belgium). In this compact **brain scanner** example, the inner imager diameter of 25 cm and 3 mm (left plot) and 1.5 mm (right plot) LYSO scintillation pixel sizes were assumed. The DOI resolution dominates the performance of the scanner. To maintain ~2–3 mm resolution in the whole brain volume in such a tight detector structure, DOI resolution should be in 2–3 mm range.

sensitivity of the system, and timing of the imaging scan (when done and for how long). To benefit from the ~1 mm range spatial resolution there has to be enough detected events during the scan to fill all the small 3D voxels in the reconstructed volumes and per each time bin (if dynamic analysis is performed). Insufficient number of events in the image voxels results in very noisy images, that cannot be utilized unless software filtering algorithms that add controlled image blurring, which is in fact negating the advantages of the intrinsically high spatial resolution. This argument can be also formulated as that achievable event statistics in fact sets the limit on the useful spatial resolution for the imaging tasks, also depending on the imaging agent.

High uptake of the specific imaging agents justifies the push for the best achievable detector performance, even if in the majority of cases the very high resolution will not be usable and the filtering of data in the processing phase, as mentioned above, will be equivalent to using system with moderate spatial resolution to start with.

However, as mentioned earlier, the practically achievable spatial resolution using the intrinsically high-resolution PET scanner, either in the clinic or even in the research center where better precautions can be taken, may still ultimately depend on how accurate is the motion correction of human subjects. Many novel approaches are investigated, with optical markerless techniques and using directly the PET scanner data leading, with sub-mm results reported [90–95].

Addendum 2: The TOF advantage

PET is converting into TOF PET to benefit from the increased sensitivity and resolution. Many papers describe the progress and discuss the future [10–16]. Just very recently, a paper was published showing first reconstructionless images obtained at 32 ps FWHM [17].

The variance reduction of a TOF-PET system over a non-TOF PET system can be computed analytically for the center of a uniform cylinder and, assuming $D >> \Delta x$, and it equals: $\frac{VAR_{nonTOF}}{VAR_{TOF}} = \frac{\sqrt{21n2}}{2a}\frac{D}{\Delta x}$, where D is the diameter of the cylinder and is the TOF spatial resolution. Therefore, the variance gain of one TOF-PET system over another is inversely proportional to the ratio of their TOF-resolutions. There is some confusion of the advantage that TOF offers due to the two different measures used to compare systems with different TOF performance. One measure is the "sensitivity", proportional to the above-defined variance gain, and the second is the Signal-to-Noise ratio (SNR) gain, expressed as square root of the variance gain. The SNR measure is a more accurate description of the practical situation in detecting image features against the noise background in the reconstructed tomographic images. For comparing scanners, SNR is thought to be a more appropriate measure. Between 200 and 400 ps, the sensitivity gain is factor 2, and SNR gain is \sqrt(2) = 1.4. There is also an additional issue how SNR is defined. Usually for detection, SNR is defined as the ratio between contrast and background noise. While contrast is important for detection, it is more related to the tracer. Due to relatively small object size, in brain imaging, the advantage of TOF is not that large, and as discussed before, it comes at a high expense and may actually cause a net sensitivity decrease due to creation of additional mechanical issues, and resultant cracks in angular coverage.

References

1. Wahl RL. Principles and practice of PET and PET/CT, 2nd ed. Philadelphia, PA: Lippincott Williams & Wilkins; 2008.
2. Lewellen TK. Recent developments in PET detector technology. Phys Med Biol 2008;53:R287–317.
3. Lewellen TK. The challenge of detector designs for PET. AJR 2010; 195:301–9.
4. Peng H, Levin CS. Recent developments in PET instrumentation. Curr Pharmaceut Biotechnol 2010;11:555–71.
5. Lee JS. Technical advances in current PET and hybrid imaging systems. Open Nucl Med J 2010;2:192–208.
6. Vaquero JJ, Kinahan P. Positron emission tomography: current challenges and opportunities for technological advances in clinical and preclinical imaging systems. Annu Rev Biomed Eng 2015:385–414. https://doi.org/10.1146/annurev-bioeng-071114-040723.
7. Guerra D, Belcari N, Bisogni M. Positron emission tomography: its 65 years. Riv Nuovo Cimento 2016;39. https://doi.org/10.1393/ncr/i2016-10122-6.
8. Walrand S, Hesse M, Jamar F. Update on novel trends in PET/CT technology and its clinical applications. Br J Radiol 2016;89.
9. Jones T, Townsend D. History and future technical innovation in positron emission tomography. J Med Imag 2017;4. https://doi.org/10.1117/1.JMI.4.1.011013.
10. Berg E, Cherry SR. Innovations in instrumentation for positron emission tomography. Semin Nucl Med 2018;48:311–31.
11. Been Han Y, Gyu Kang H, Hyun Song S, Bae Ko G, Sung Lee J, Jong Hong S. SiPM-based dual-ended-readout DOI-TOF PET module based on mean-time method. J Instrum 2019;14. https://doi.org/10.1088/1748-0221/14/02/p02023.
12. Surti S. Update on time-of-flight PET imaging. J Nucl Med 2015; 56:98–105.
13. Surti S, Karp JS. Advances in time-of-flight PET. Phys Med 2016; 32:12–22.
14. Cates JW, Levin CS. Advances in coincidence time resolution for PET. Phys Med Biol 2016;61:2255.

15. Vandenberghe S, Mikhaylova E, D'Hoe E, Mollet P, Karp JS. Recent developments in time-of-flight PET. EJNMMI Phys 2016;3:3.
16. Seifert S, Schaart DR. Improving the time resolution of TOF-PET detectors by double-sided readout. IEEE Trans Nucl Sci 2015;62: 3–11.
17. Kwon SI, Roncali E, Gola A, Paternoster G, Piemonte C, Cherry SR. Dual-ended readout of bismuth germanate to improve timing resolution in time-of-flight PET. Phys Med Biol 2019;64:105007.
18. Kwon SI, Ota R, Berg E, Hashimoto F, Nakajima K, Ogawa I, et al. Ultrafast timing enables reconstruction-free positron emission imaging. Nat Photonics 2021;15:914–8.
19. Phelps ME. PET: the merging of biology and imaging into molecular imaging. J Nucl Med 2000;41:661–81.
20. Carson RE, Kuo PH. Brain-dedicated emissio tomography systems: a perspective on requirements for clinical research and clinical needs in brain imaging. IEEE Trans Radiat Plasma Med Sci 2019;3:254–61.
21. Hooker JM, Carson RE. Human positron emission tomography neuroimaging. Annu Rev Biomed Eng 2019;21:551–81.
22. Laruelle M. Imaging synaptic neurotransmission with in vivo binding competition techniques: a critical review. J Cereb Blood Flow Metab 2000;20:423–51.
23. Fung EK, Carson RE. Cerebral blood flow with [15O]water PET studies using an image-derived input function and MR-defined carotid centerlines. Phys Med Biol 2013;58:1903–23.
24. Faul M, Coronado V. Epidemiology of traumatic brain injury. In: Handbook of clinical neurology, vol 127. Elsevier; 2015: 3–13 pp.
25. Morbelli S, Garibotto V, Van De Giessen E, Arbizu J, Chetelat G, Drezgza A, et al. A Cochrane review on brain [18F]FDG PET in dementia: limitations and future perspectives. Eur J Nucl Med Mol Imaging 2015;42:1487–91.
26. Finnema SJ, Nabulsi NB, Eid T, Detyniecki K, Lin SF, Chen MK, et al. Imaging synaptic density in the living human brain. Sci Transl Med 2016;8:348ra96.
27. Kelley P, Evans MDR, Kelley J. Making memories: why time matters. Front Hum Neurosci 2018;12:400.
28. Chen MK, Mecca AP, Naganawa M, Finnema SJ, Toyonaga T, Lin SF, et al. Assessing synaptic density in Alzheimer disease with synaptic vesicle glycoprotein 2A positron emission tomographic imaging. JAMA Neurol 2018;75:1215–24.
29. Funck T, Palomero-Gallagher N, Omidyeganeh M, Lepage C, Toussaint PJ, Khalili N, et al. Towards a gold standard for validation of quantification methods for PET neuroreceptor imaging. In: 29th international symposium on cerebral blood flow, metabolism and function; 2019: Journal of Cerebral Blood Flow & Metabolism.
30. Molnar Z, Clowry GJ, Sestan N, Alzu'bi A, Bakken T, Hevner RF, et al. New insights into the development of the human cerebral cortex. J Anat 2019;235:432–51. [Epub 2019/08/03].
31. Surti S, Karp J. Impact of detector design on imaging performance of a long axial field-of-view, whole-body PET scanner. Phys Med Biol 2015;60:5343.
32. Zhang XZ, Zhou J, Cherry SR, Badawi RD, Qi JY. Quantitative image reconstruction for total-body PET imaging using the 2-meter long EXPLORER scanner. Phys Med Biol 2017;62: 2465–85.
33. Zhang X, Zhou J, Cherry SR, Badawi RD, Qi J. Quantitative image reconstruction for total-body PET imaging using the 2-meter long EXPLORER scanner. Phys Med Biol 2017;62:2465–85.
34. Cherry SR, Badawi RD, Karp JS, Moses WW, Price P, Jones T. Total-body imaging: transforming the role of positron emission tomography. Sci Transl Med 2017;9:eaaf6169.
35. Cherry SR, Jones T, Karp JS, Qi J, Moses WW, Badawi RD. Total-body PET: maximizing sensitivity to create new opportunities for clinical research and patient care. J Nucl Med 2018;59: 3–12.
36. Leung EK, Judenhofer MS, Cherry SR, Badawi RD. Performance assessment of a software-based coincidence processor for the EXPLORER total-body PET scanner. Phys Med Biol 2018;63: 18NT01.
37. Berg E, Zhang X, Bec J, Judenhofer MS, Patel B, Peng Q, et al. Development and evaluation of mini-EXPLORER: a long axial field-of-view PET scanner for nonhuman primate imaging. J Nucl Med 2018;59:993–8.
38. Badawi RD, Shi H, Hu P, Chen S, Xu T, Price PM, et al. First human imaging studies with the EXPLORER total-body PET scanner. J Nucl Med 2019;60:299–303.
39. Zhang X, Xie Z, Berg E, Judenhofer MS, Liu W, Xu T, et al. Total-body dynamic reconstruction and parametric imaging on the uEXPLORER. J Nucl Med 2019;61:285–91. [Epub 2019/07/16].
40. Zhang X, Xie Z, Berg E, Judenhofer M, Liu W, Lv Y, et al. Total-body parametric imaging using kernel and direct reconstruction on the uEXPLORER. J Nucl Med 2019;60(1 Suppl):456.
41. Zhang X, Cherry S, Badawi R, Qi J. Total-body dynamic PET imaging with 100-ms temporal resolution. Montreal, QC, Canada: World Molecular Imaging Congress; 2019.
42. Deng Z, Hu D, Ding Y, Dong Y. A comparison of image quality with uMI780 and the first total-body uEXPLORER scanner. J Nucl Med 2019;60(1 Suppl):381.
43. Karp JS, Vishwanath V, Geagan M, Muehllehner G, Pantel A, Parma M, et al. PennPET explorer: design and preliminary performance of a whole-body imager. J Nucl Med June 2019;21. https://doi.org/10.2967/jnumed.119.229997.
44. Pantel AR, Viswanath V, Daube-Witherspoon ME, Dubroff JG, Muehllehner G, Parma MJ, et al. Human imaging on a whole-body imager. J Nucl Med 2019. https://doi.org/10.2967/jnumed.119.231845.
45. Viswanath V, Daube-Witherspoon M, Karp J, Surti S. Lesion detectability in long axial field of view TOF PET scanners. J Nucl Med 2019;60(1 Suppl):107.
46. Lyu Y, Lv X, Liu W, Judenhofer MS, Zwingenberger A, Wisner ER, et al. Mini EXPLORER II: a prototype high-sensitivity PET/CT scanner for companion animal whole body and human brain scanning. Phys Med Biol 2019;64. https://doi.org/10.1088/1361-6560/aafc6c.
47. [D] Vandenberghe S, Moskal P, Karp JS. State of the art in total body PET. EJNMMI Phys 2020;7:35.
48. Moliner L, Rodríguez-Alvarez MJ, Catret JV, González A, Ilisie V, Benlloch JM. NEMA performance evaluation of CareMiBrain dedicated brain PET and comparison with the whole body and dedicated brain PET systems. Sci Rep 2019:9;15484.
49. Tashima H, Yamaya T. Proposed helmet PET geometries with add-on detectors for high sensitivity brain imaging. Phys Med Biol 2016;61:7205–20.
50. Ahmed AM, Tashima H, Yoshida E, Nishikido F, Yamaya T. Simulation study comparing the helmet-chin PET with a cylindrical PET of the same number of detectors. Phys Med Biol 2017;62:4541–50.

51. Ahmed M, Tashima H, Yoshida E, Yamaya T. Investigation of the optimal detector arrangement for the helmet-chin PET – a simulation study. Nucl Instrum Methods Phys Res A 2017;858: 96–100.
52. Gong K, Majewski S, Kinahan PE, Harrison RL, Elston BF, Manjeshwar R, et al. Designing a compact high performance brain PET scanner-simulation study. Phys Med Biol 2016;61: 3681–97.
53. Schmidtlein CR, Turner JN, Thompson MO, Mandal KC, Haggstrom I, Zhang J, et al. Performance modeling of a wearable brain PET (BET). In: Proceedings SPIE. San Diego, USA: SPIE; 2016:9788 p.
54. Schmidtlein CR, Turner JN, Thompson MO, Mandal KC, Haggstrom Zhang J, Humm JL, et al. Initial performance studies of a wearable brain positron emission tomography camera based on autonomous thin-film digital Geiger avalanche photodiode arrays. J Med Imaging 2017;4:011003.
55. Moskal P, Kowalski P, Shopa RY, Raczyński L, Baran J, Chug N, et al. Simulating NEMA characteristics of the modular total-body J-PET scanner—an economic total-body PET from plastic scintillators. Phys Med Biol 2021;66:175015.
56. Tai YC, Wu H, Pal D, O'Sullivan JA. Virtual-pinhole PET. J Nucl Med 2008;49:471–9.
57. Jiang J, Samanta S, Li K, Siegel SB, Mintzer RA, Cho S, et al. Augmented whole-body scanning via magnifying PET. IEEE Trans Med Imaging 2020;39:3268–77.
58. Jiang J, Li K, Wang Q, Puterbaugh K, Young JW, Siegel SB, et al. A second-generation virtual-pinhole PET device for enhancing contrast recovery and improving lesion detectability of a whole-body PET/CT scanner. Med Phys 2019;46:4165–76.
59. Jiang J, Samanta S, Li K, Hamdi M, Siegel SB, Mintzer R, et al. Augmented whole-body scanning via magnifying PET. J Nucl Med 2020;61(1 Suppl):309.
60. Zhou J, Qi J. Theoretical analysis and simulation study of a high-resolution zoom-in PET system. Phys Med Biol 2009;54:5193.
61. Zhou J, Qi J. Adaptive imaging for lesion detection using a zoom-in PET system. IEEE Trans Med Imag 2010;30:119–30.
62. Carson R, Berg E, Ramsey B, Cherry S, Du J, Tao F, et al. Design of the NeuroEXPLORER, a next-generation ultra-high performance human brain PET imager. J Nucl Med 2021;62(1 Suppl):1120.
63. Soret M, Bacharach SL, Buvat I. Partial-volume effect in PET tumor imaging. J Nucl Med 2007;48:932–45.
64. Guillette N, Sarrhini O, Lecomte R, Bentourkia M. Correction of partial volume effect in the projections in PET studies. Conference: IEEE Nuclear Science Symposium 2010:3541–3. https://doi.org/10.1109/NSSMIC.2010.5874467.
65. Erlandsson K, Buvat I, Pretorius PH, Thomas BA, Hutton BF. A review of partial volume correction techniques for emission tomography and their applications in neurology, cardiology and oncology. Phys Med Biol 2012;57:R119–59.
66. Cysouw MCF, Golla SVS, Frings V, Smit EF, Hoekstra OS, Kramer GM, et al. Partial-volume correction in dynamic PET-CT: effect on tumor kinetic parameter estimation and validation of simplified metrics. EJNMMI Res 2019;9:12.
67. Yang J, Hu C, Guo N, Dutta J, Vaina LM, Johnson KA, et al. Partial volume correction for PET quantification and its impact on brain network in Alzheimer's disease. Sci Rep 2017;7:13035.
68. Wienhard K, Schmand M, Casey M, Baker K, Bao J, Eriksson L, et al. The ECAT HRRT: performance and first clinical application of the new high resolution research tomograph. IEEE Trans Nucl Sci 2002;49:104–10.
69. Eriksson L, Wienhard K, Eriksson M, Casey ME, Knoess C, Bruckbaer T, et al. The ECAT HRRT: NEMA NEC evaluation of the HRRT system, the new high-resolution research tomograph. IEEE Trans Nucl Sci 2002;49:2085–8.
70. VanVelden FH, Kloet RW, van Berckel BN, Buijs FL, Luurtsema G, Lammertsma AA, et al. HRRT versus HR+ human brain PET studies: an interscanner test–retest study. J Nucl Med 2009;50:693–702.
71. Yamaya T, Yoshida E, Obi T, Ito H, Yoshikawa K, Murayama H. First human brain imaging by the jPET-D4 prototype with a pre-computed system matrix. IEEE Trans Nucl Sci 2008;55:2482–92.
72. Z Wang, W Yu, S Xie. A dedicated PET system for human brain and head/neck imaging, published in: 2013 IEEE Nuclear Science Symposium and Medical Imaging Conference (2013 NSS/MIC), https://doi.org/10.1109/NSSMIC.2013.6829112.
73. NeuroPET/CT PhotoDiagnostic systems. Available from: https://www.photodiagnostic.com/petct.
74. Grogg KS, Toole T, Ouyang J, Zhu X, Normandin M, Johnson K, et al. NEMA and clinical evaluation of a novel brain PET-CT scanner. J Nucl Med 2016;57:646–52.
75. CerePET. Brain biosciences. Available from: https://www.linkedin.com/company/brain-biosciences-inc.
76. Gómez Herrero JA, Navarro García J, Carlos M, Vicente A, José L, Serra P, et al. Development of a new device for the early diagnosis of Alzheimer's disease. Rev Biomechan. http://www.biomecanicamente.org/item/1159-rb65-caremibrain-english.html?tmpl=component&print=1.
77. CareMiBrain imager, ONCOVISION, Valencia, Spain, https://www.oncovision.com.
78. Gaudin E, Toussaint M, Thibaudeau C, Fontaine R, Normandin M, Petibon Y, et al. Simulation studies of the SAVANT high resolution dedicated brain PET scanner using individually coupled APD detectors and DOI encoding. J Nucl Med 2019;60:531.
79. NeuroLF, Positrigo. Available from: https://www.positrigo.com/.
80. Bläckberg L, Sanchez D, Borghi G, Ballabriga R, Sajedi S, Gómez S, et al. High sensitivity and high resolution dynamic brain-dedicated TOF-DOI PET scanner. In: 2020 IEEE Nuclear Science Symposium and Medical Imaging Conference (NSS/MIC). 978-78-1-7281-7693-2/20. https://doi.org/10.1109/NSS/MIC42677.2020.9507837.
81. Gaudin E, Toussaint M, Thibaudeau C, Paille M, Fontaine R, Lecomte R. Performance simulation of an ultra-high resolution brain PET scanner using 1.2 mm pixel detectors. IEEE Trans Radiat Plasma Med Sci 2019;3:334–42.
82. Organ specific PET, prescient imaging. Available from: http://prescient-imaging.com/.
83. González AJ, Majewski S, Sánchez F, Aussenhofer S, Aguilar A, Conde P, et al. The MINDView brain PET detector, feasibility study based on SiPM arrays. Nucl Instrum Methods Phys Res 2016;818:82–90.
84. Benlloch JM, González AJ, Pani R, Preziosi E, Jackson C, Murphy J, et al. The MINDVIEW project: first results. Eur Psychiatry 2018. https://doi.org/10.1016/j.eurpsy.2018.01.002.
85. Lecoq P. Pushing the limits in time-of-flight PET imaging. IEEE Trans Radiat Plasma Med Sci 2017;1. https://doi.org/10.1109/trpms.2017.2756674.
86. Prior J. The 10-ps TOF PET: clinical applications, presented at the FATA2019: FAst Timing Applications for nuclear physics and medical imaging, 3–5 September 2019, Accademia degli Zelanti e dei Dafnici. Catania, Italy: Acireale. https://agenda.infn.it/event/18991/timetable/.

87. Gasper Razdevsek P, Dolenec R, Peter K, Majewski S, Studen A, Korpar S, et al. Multi-panel limited angle PET system with 50 ps FWHM coincidence time resolution: a simulation study. accepted for publication in Trans Radiat Plasma Med Sci 2021: 2021. https://doi.org/10.1109/TRPMS.2021.3115704.
88. Harmon ES, Thompson MO, Ross Schmidtlein C, Turner JN, Krol A. Towards 50 ps TOF-PET for brain imaging. Proc. SPIE 10953, Medical Imaging 2019: Biomedical Applications in Molecular, Structural, and Functional Imaging 2019:1095303. https://doi.org/10.1117/12.2515123.
89. The Siemens Biograph vision PET/CT. https://www.siemens-healthineers.com/en-us/molecular-imaging/pet-ct/biograph-vision.
90. van Sluis J, de Jong J, Schaar J, Noordzij W, van Snick P, Dierckx R, et al. Performance characteristics of the digital Biograph Vision PET/CT system. J Nucl Med 2019. https://doi.org/10.2967/jnumed.118.215418.
91. Kyme AZ, Se S, Meikle SR, Fulton RR. Markerless motion estimation for motion-compensated clinical brain imaging. Phys Med Biol 2018;63:105018.
92. Lu Y, Gallezot JD, Naganawa M, Fontaine K, Toyonaga T, Ren S, et al. Data-driven motion detection and event-by-event correction for brain PET. J Nucl Med. 2018;59(1 Suppl).
93. Lu Y, Gallezot JD, Naganawa M, Ren S, Fontaine K, Wu J, et al. Data-driven voluntary body motion detection and non-rigid event-by-event correction for static and dynamic PET. Phys Med Biol 2019;64:065002.
94. Ren S, Lu Y, Bertolli O, Thielemans K, Carson RE. Event-by-event non-rigid data-driven PET respiratory motion correction methods: comparison of principal component analysis and centroid of distribution. Phys Med Biol 2019;64:165014.
95. Sun C, Fontaine K, Revilla E, Toyonaga T, Gallezot JD, Mulnix T, et al. A data-driven quality control method for head motion tracking in PET. IEEE NSS/MIC. 2019.
96. Hurley S, Spangler-Bickell M, Deller T, Bradshaw T, Jansen F, McMillan A. Data-driven rigid motion correction of PET brain images using list mode reconstruction. J Nucl Med 2019;60 (1 Suppl):1358.
97. Shi H, Du D, Xu J, Peng Q. Assessment of dedicated brain PET designs with different geometries. IEEE MIC; 2013.
98. Shi H, Du D, Xu J, Peng Q. PMT based pentagonal and hexagonal detector module designs for convex polyhedron PET systems. IEEE MIC; 2013.
99. Han S, Dong Du, Xu JF, Su Z, Peng Q. Design study of dedicated brain PET with polyhedron geometry. Technol Health Care 2015; 23:S615–23.
100. Xu JF, Huang Q, Weng F, Zan Y, Chen J, Xie S, et al. Progresses in designing a high-sensitivity dodecahedral PET for brain imaging, nuclear science symposium. In: Medical Imaging Conference and Room-Temperature Semiconductor Detector Workshop (NSS/MIC/RTSD); 2016.
101. Derenzo SE, Choong W-S, Moses WW. Monte Carlo calculations of PET coincidence timing: single and double-ended readout. Phys Med Biol 2015;60:7309.
102. Derenzo SE. Monte Carlo simulations of time-of-flight PET with double-ended readout: calibration, coincidence resolving times and statistical lower bounds. Phys Med Biol 2017;62: 3828–58.
103. Philadelphia SSS, Karp JS. Limited angle tomography with time-of-flight PET; 2014. US Patent US 8,698,087 B2, Apr. 15.
104. Cal-Gonzalez J, Rausch I, Lalith K, Sundar S, Lassen ML, Muzik O, et al. Hybrid imaging: instrumentation and data processing. Front Phys 2018:6. Article 47.https://doi.org/10.3389/fphy.2018.00047. www.frontiersin.org.
105. Hong KJ, Ho Jung YCJ, Kang J, Hu W, Lim HK, Huh Y, et al. A prototype MR insertable brain PET using tileable GAPD arrays. Med Phys 2013;40. https://doi.org/10.1118/1.4793754.
106. González AJ, Conde P, Hernández L, Herrero V, Moliner L, Monzó JM, et al. Design of the PET-MR system for head imaging of the DREAM project. Nucl Instrum Methods 2013;702:94–7.
107. Cho G, Choi Y, Sung Lee J, An HJ, Jung JH, Park HW, et al. Preliminary evaluation of a brain PET insertable to MRI. EJNMMI Phys 2014;1(1 Suppl):A13. http://www.ejnmmiphys.com/content/1/S1/A13.
108. Galve P, Catana C, Herraiz JL, Udía JM. GPU based fast and flexible iterative reconstructions of arbitrary and complex PET scanners: application to next generation dedicated brain scanners. In: M-03 – 2020 IEEE NSS-MIC conference.
109. Catana C. Development of dedicated brain PET imaging devices – recent advances and future perspectives. J Nucl Med 2019. https://doi.org/10.2967/jnumed.118.217901.
110. Nakamoto R, Nakamoto Y, Ishimori T, Fushimi Y, Kido A, Togashi K. Comparison of PET/CT with sequential PET/MRI using an MR-compatible mobile PET system. J Nucl Med 2017;2. https://doi.org/10.2967/jnumed.117.197665.
111. Vaska P, Woody CL, Schlyer DJ, Shokouhi S, Stoll SP, Pratte JF, et al. RatCAP: miniaturized head-mounted PET for conscious rodent brain imaging. IEEE Trans Nucl Sci 2004;51:2718–22.
112. Majewski S, Proffitt J. 2011. Compact and mobile high resolution PET brain imager. US Patent. 7,884,331.
113. Majewski S, Proffitt J, Brefczynski-Lewis J, Stolin A, Weisenberger AG, Xi W, et al. A silicon photomultiplier based wearable brain imager. In: Proceedings of the IEEE Nuclear Science Symposium and Medical Imaging Conference Record, Valencia, Spain, 23–29 October 2011. 4030–4 pp.
114. Bauer CE, Brefczynski-Lewis J, Marano G, Mandich M-B, Stolin A, Martone P, et al. Concept of an upright wearable positron emission tomography imager in humans. Brain Behav 2016;00: 1–10: e00530.
115. Melroy S, Bauer C, McHugh M, Carden G, Stolin A, Majewski S, et al. Development and design of next-generation head-mounted ambulatory microdose positron-emission tomography (AM-PET) system. Sensors 2017;17:1164.
116. Majewski S and Brefczynski-Lewis J. VIRPET – combination of virtual reality and PET brain imaging, US Patent 9,655,573, 2017.
117. Noble RM. Ambulatory microdose PET: a wearable PET scanner for neurologic imaging. J Nucl Med Technol 2019;47. https://doi.org/10.2967/jnmt.119.228718.
118. Volkow N. presentation at the BRAIN initiative workshop: transformative non-invasive imaging technologies. 2021. https://www.youtube.com/watch?v=A2p1oznwo6Y NIH Brain Initiative Transformative.
119. Non-invasive imaging technologies workshop. 2021. https://videocast.nih.gov/watch=40183.
120. Yoshida E, Tashima K, Nagatsu K, Tsuji AB, Kamada K, Parodi K, et al. Whole gamma imaging: a new concept of PET combined with Compton imaging. Phys Med Biol 2020;65:125013.
121. Yoshida E, Tashima H, Nagatsu K, Tsuji AB, Kamada K, Parodi K, et al. Whole gamma imaging: a new concept of PET combined with Compton imaging. Phys Med Biol 2020;65:125013.

122. Tashima H, Yoshida E, Wakizaka H, Takahashi M, Nagatsu K, Tsuji AB, et al. Development of a hybrid image reconstruction algorithm combining PET and compton events for whole gamma imaging. In: 2020 IEEE Nuclear Science Symposium and Medical Imaging Conference (NSS/MIC). https://doi.org/10.1109/NSS/MIC42677.2020.9507841.
123. Moskal P, Stępień EŁ. Prospects and clinical perspectives of total-body PET imaging using plastic scintillators. Pet Clin 2020; 15:439–52.
124. Moskal P, Krawczyk N, Hiesmayr BC, Bala M, Curceanu C, Czerwiński E, et al. Feasibility studies of the polarization of photons beyond the optical wavelength regime with the J-PET detector. Eur Phys J C 2018;78:970.
125. Moskal P, Kisielewska D, Curceanu C, Czerwińska E, Dulski K, Gajos A, et al. Feasibility study of the positronium imaging with the J-PET tomograph. Phys Med Biol 2019. https://doi.org/10.1088/1361-6560/aafe20.
126. Moskal P. Positronium imaging. In: 2019 IEEE Nuclear Science Symposium and Medical Imaging Conference (NSS/MIC) (IEEE, 2019). 1–3 pp. https://doi.org/10.1109/NSS/MIC42101.2019.9059856.
127. Moskal P, Jasińska B, Stępień EŁ, Bass SD. Positronium in medicine and biology. Nat Rev Phys 2019;1:527–9.
128. Moskal P, Dulski K, Chug N, Curceanu C, Czerwiński E, Dadgar M, et al. Positronium imaging with the novel multiphoton PET scanner. Sci Adv 2021;7. https://doi.org/10.1126/sciadv.abh4394.
129. Moskal P, Gajos A, Mohammed M, Chhokar J, Chung N, Curceanu C, et al. Testing CPT symmetry in ortho-positronium decays with positronium annihilation tomography. Nat Commun 2021;12:5658.
130. Stępień E, Kubicz E, Grudzień G, Dulski K, Leszczyński B, Moskal P. Positronium life-time as a new approach for cardiac masses imaging. Eur Heart J 2021;42(1 Suppl). https://doi.org/10.1093/eurheartj/ehab724.3279.
131. Jasińska B, Moskal P. A new PET diagnostic indicator based on the ratio of 3gamma/2gamma positron annihilation. Acta Phys Pol B 2017;48:1737.
132. Godinez PF, Gong K, Zhou J, Judenhofer MS, Chaudhari AJ, Badawi RD. Development of an ultra high resolution PET scanner for imaging rodent paws: PawPET. IEEE Trans Radiat Plasma Med Sci 2018;2. https://doi.org/10.1109/TRPMS.2017.2765486.
133. Gaudin E, Thibaudeau C, Arpin L, Fontaine R, Lecomte R. Imaging performance of a submillimetric spatial resolution APD-based preclinical PET scanner dedicated to mouse imaging. Atlanta: presented at the IEEE MIC; 2017:21–8 pp.
134. Yamamoto S, Watabe H, Watabe T, Ikeda H, Kanai Y, Ogata Y, et al. Development of ultrahigh resolution Si-PM-based PET system using 0.32 mm pixel scintillators. Nucl Instrum Methods Phys Res 2016;836:7–12.
135. Moses WW. Fundamental limits of spatial resolution in PET. Nucl Instrum Methods Phys Res 2011;648(Suppl):S236–40.
136. Niknejad T, Pizzichemi M, Stringhini G, Auffray E, Bugalho R, Silva JCD, et al. Development of high-resolution detector module with depth of interaction identification for positron emission tomography. Nucl Instrum Methods Phys Res Sect A Accel Spectrom Detect Assoc Equip 2017;845(C Suppl):684–8. https://doi.org/10.1016/j.nima.2016.04.080 http://www.sciencedirect.com/science/article/pii/S0168900216302935.
137. Du J, Bai X, Gola A, Acerbi F, Ferri A, Piemonte C, et al. Performance of a high-resolution depth-encoding PET detector module using linearly-graded SiPM arrays. Phys Med Biol 2018;63:035035.
138. Du J, Bai X, Cherry SR. Performance comparison of depth-encoding detectors based on dual-ended readout and different SiPMs for high-resolution PET applications. Phys Med Biol 2019; 64:15NT03.